Nonlocal momentum transfer in *welcher Weg* measurements

H. M. Wiseman,[1,2] F. E. Harrison,[1,2] M. J. Collett,[1] S. M. Tan,[1] D. F. Walls,[1] and R. B. Killip[3]
[1]*Department of Physics, University of Auckland, Auckland, New Zealand*
[2]*Department of Physics, University of Queensland, Queensland 4072, Australia*
[3]*Department of Mathematics, University of Auckland, Auckland, New Zealand*
(Received 29 February 1996; revised manuscript received 31 December 1996)

A ''which-path'' (*welcher Weg*) measurement necessarily destroys the fringes in a double-slit interference experiment. We show that in all instances one may attribute this destruction to a disturbance of the particle's momentum by an amount equal to at least $\pi\hbar/2d$, where d is the slit separation, in accordance with the uncertainty principle. However, this momentum transfer need not be local; that is, it need not act at either of the slits through which the particle passes. For well-known *welcher Weg* measurements such as Einstein's recoiling slit and Feynman's light microscope, the disturbance can be understood in terms of random classical momentum kicks that act locally. In some recent proposals, including that by Scully, Englert, and Walther [Nature (London) **351**, 111 (1991)], the momentum transfer is of a peculiarly quantum, nonlocal nature. In this paper we introduce a formalism based on the Wigner function, as this describes both the local and nonlocal momentum transfer caused by any *welcher Weg* measurement. We show that for some examples, such as that of Scully, Englert, and Walther, there is no momentum disturbance at the slits even though the nonlocal momentum disturbance is sufficient to destroy the interference pattern. Finally, we discuss the experimental signatures of nonlocal versus local momentum transfer and demonstrate a strong similarity to the nonlocality of the Aharonov-Bohm effect. [S1050-2947(97)04006-7]

PACS number(s): 03.65.Bz, 03.75.Dg, 42.50.Vk, 32.80.Lg

I. INTRODUCTION

Making a position measurement to determine which way a particle goes through a double-slit apparatus necessarily destroys the interference pattern. This is the canonical example of Bohr's complementarity principle [1]. In well-known *welcher Weg* ''which-path'' experiments, such as Einstein's recoiling slit [1] and Feynman's light microscope [2], the destruction of interference can be explained in terms of uncontrolled classical momentum kicks to the particle. Bohr used this simple picture in his debates with Einstein to show how the uncertainty principle enforced complementarity [1]. In recent years, interest in this topic has been rekindled by a *welcher Weg* measurement scheme proposed by Scully and co-workers [3–5]. They claim that their scheme destroys the interference without transferring any transverse momentum to the particle. Storey and co-workers [4–6] have argued to the contrary that whenever interference is destroyed, transverse momentum is transferred in line with the uncertainty principle.

In considering whether or not momentum is transferred it is essential to define exactly what constitutes a momentum transfer. Unless explicitly stated otherwise, all the momentum transfers discussed in this paper are in the transverse direction. As Wiseman and Harrison noted recently [7], there are (at least) two different but reasonable ways of defining a random momentum transfer. The first definition corresponds to the classical notion of a convolution of the particle's momentum probability distribution with a momentum transfer *probability* distribution. The ensemble of random classical momentum kicks would result in the smearing of the momentum distribution of the particle. The second definition corresponds to the more quantum-mechanical idea of a convolution of the particle's momentum wave function with a set of momentum transfer *amplitude* distributions. In general, a set of quantum momentum transfer amplitude distributions cannot be recast as a classical probability distribution for momentum kicks. Unlike classical momentum kicks, the effect of a quantum momentum transfer on a particle's momentum distribution will in general depend on its initial wave function.

As noted above, in traditional double-slit *welcher Weg* measurements the loss of fringe visibility may be ascribed to classical momentum kicks. Because of their classical nature, these momentum kicks would have an identical effect on the momentum distribution of a particle passing through a single slit. That is to say, the single-slit diffraction pattern would be smeared in the same way as the double-slit interference pattern. Scully *et al.* showed that in their proposed scheme there would be no broadening of the single-slit diffraction pattern. This is the basis for their claim that there is no momentum transfer in their scheme, a claim that is valid if one has in mind the first (classical) concept of momentum kicks.

Although the scheme of Scully *et al.* shows that Bohr's naive classical realist argument is not of general applicability, it does not necessarily mean that the loss of interference cannot be accounted for by random momentum transfer. Storey *et al.* have shown, by means of a general theorem, that loss of interference requires that there be some amplitude for a quantum momentum transfer in accordance with the uncertainty principle. This result is not in conflict with the conclusion of Scully *et al.* because quantum momentum transfers do not imply classical momentum kicks. In particular, in a quantum or nonclassical *welcher Weg* scheme there need not be any disturbance of the diffraction pattern of a single slit even though the interference pattern of a double slit is destroyed by a quantum momentum transfer.

For both classical and quantum *welcher Weg* schemes the

origin of the momentum transfer is in the interaction between the particle and the *welcher Weg* measuring apparatus. In the scheme of Scully *et al.*, this is an interaction between an atom and a microwave cavity field. As we shall show, the momentum transfer in this case is of a peculiarly quantum, nonlocal nature. In their analysis Storey *et al.* described this momentum transfer as ''the repeated emission and reabsorption of microwave photons by the atom'' [4]. We have avoided using this simple physical picture in the present paper because it may give the false impression that one can understand the momentum transfer in terms of localized classical momentum kicks.

In this paper we investigate further the distinction between quantum and classical momentum kicks. In order to be able to treat them on the same footing, we adopt the Wigner function formalism. This enables us to define a momentum transfer Wigner function $W_T(x,p)$. Formally this plays the role of the probability distribution for a particle at position x to receive a momentum transfer of p, although $W_T(x,p)$ need not be everywhere positive. We find that the smearing of the diffraction pattern and the destruction of the interference fringes are determined by different momentum transfers. That is, the distributions for these momentum transfers are given by different parts of the momentum transfer Wigner function. The smearing is determined by $W_T(x,p)$ for x at the positions of the slits. We call this the *local* momentum transfer distribution $P_{\rm local}(p)$. The destruction of interference is determined by $W_T(x,p)$ for x midway between the slits, where the particle is never found. We call this the *nonlocal* momentum transfer distribution $P_{\rm nonlocal}(p)$. It is this nonlocal momentum transfer that cannot be less than that required by the uncertainty principle.

For classical momentum kicks, $W_T(x,p)$ is independent of x and positive semidefinite, which means that the particle receives a classical random momentum kick independent of its initial state. In this case $W_T(x,p)=P_{\rm local}(p)=P_{\rm nonlocal}(p)$ and the destruction of interference is accompanied by local momentum kicks, which necessarily smear the diffraction pattern. For nonclassical *welcher Weg* schemes, $W_T(x,p)$ varies with x and the destruction of interference cannot be attributed to local momentum kicks. The scheme of Scully *et al.* is a case in point. Although $P_{\rm local}(p)$ transfers no momentum locally, $P_{\rm nonlocal}(p)$ does transfer momentum in accordance with the uncertainty principle, thereby effacing the interference fringes. Thus, by using the Wigner function formalism we are able to see both the absence of local momentum kicks (as shown by Scully *et al.*) and the presence of a nonlocal momentum transfer (which satisfies the theorem of Storey *et al.*).

We begin the body of the paper with a review of the distinction between classical and quantum (nonclassical) momentum transfers. In Sec. III we introduce the Wigner function description of momentum transfers in general and in the double-slit experiment in particular. We also derive a stronger lower bound on the momentum disturbance needed to destroy the double-slit interference pattern. In Sec. IV we use the Wigner function to analyze three examples of *welcher Weg* schemes explicable by classical momentum kicks. In Sec. V we do the same for four nonclassical schemes in which the destruction of interference has no local explanation. In one of these examples $W_T(x,p)$ is non-negative and yet the local momentum transfer is unequivocally zero. In Sec. VI we discuss experimental signatures of local and nonlocal momentum transfers and show that there exists a strong analogy between nonclassical *welcher Weg* schemes and Aharonov-Bohm experiments.

II. CLASSICAL AND QUANTUM MOMENTUM TRANSFERS

We shall be considering a number of experiments in which double-slit interference patterns are destroyed by making a position measurement on the particle so as to determine which slit it passed through. The slits are taken to be parallel and separated in the x direction. In order to provide a unified treatment of all cases, we follow Ref. [6] in defining the effect of a generalized position measurement on a particle's wave function to be

$$\psi_\xi(x)=N_\xi^{-1/2}O_\xi(x)\psi_i(x). \tag{2.1}$$

Here ψ_i is the initial wave function, ψ_ξ is the final wave function given the result ξ, where ξ parametrizes a set of functions $O_\xi(x)$, which is complete in the sense

$$\sum_\xi |O_\xi(x)|^2=1 \quad \forall x, \tag{2.2}$$

and N_ξ is the normalization factor

$$N_\xi=\int dx|O_\xi(x)\psi_i(x)|^2, \tag{2.3}$$

where we are using the convention that the range of all integrals is the real line unless otherwise indicated. The factor (2.3) is just the probability that the result ξ is obtained. An arbitrary wave function $\psi(x)$ can be transformed to the momentum representation as

$$\tilde{\psi}(p)=\frac{1}{\sqrt{2\pi\hbar}}\int dx\ \psi(x)e^{ipx/\hbar}. \tag{2.4}$$

In this representation Eq. (2.1) becomes

$$\tilde{\psi}_\xi(p)=(2\pi\hbar N_\xi)^{-1/2}\int dp'\tilde{\psi}_i(p-p')\tilde{O}_\xi(p'). \tag{2.5}$$

That is to say, the initial momentum wave function $\tilde{\psi}_i(p)$ is convolved with $\tilde{O}_\xi(p)$ to give the final momentum wave function $\tilde{\psi}_\xi(p)$. For this reason we call $\tilde{O}_\xi(p)$ the momentum transfer amplitude distribution for the result ξ.

This definition of position measurements encompasses all nondemolition [8] measurements of x that preserve purity [9]. A measurement preserves purity if, for an initial pure state, the final state conditioned upon any particular measurement result is also a pure state. This describes, in essence, all of the position measurements made in *welcher Weg* schemes, be they projective or not. Even if not projective, the measurements we are describing here do not represent any significant extension of the traditional quantum theory of measurement based on projective measurements. This is because these nonprojective measurements of the system can always be cast as projective measurements of the apparatus, with the

latter treated as a quantum-mechanical system [9]. In many experiments in quantum optics it is necessary to do this as the apparatus is sufficiently well isolated from external disturbance that the experimenter may choose the basis in which to observe the apparatus. Different choices of apparatus observable will result in different basis sets O_ξ, O'_η, related to each other by $O_\xi = \Sigma_\eta U_{\eta\xi} O'_\eta$, where the coefficients $U_{\eta\xi}$ satisfy

$$\sum_\eta U_{\eta\xi} U^*_{\eta\zeta} = \delta_{\xi\zeta}. \tag{2.6}$$

For any choice of apparatus basis, if a measurement is made and the result ignored, then the final state of the particle is

$$\rho_f(x,x') = \sum_\xi N_\xi \psi_\xi(x) \psi^*_\xi(x')$$

$$= \sum_\xi O_\xi(x) \psi_i(x) \psi^*_i(x') O^*_\xi(x'). \tag{2.7}$$

This is a mixed state, with a nonunique decomposition into pure state components. Using the relation (2.6) it is easy to verify that it is independent of the apparatus basis O_ξ chosen to make the measurement. That is to say, we can also write

$$\rho_f(x,x') = \sum_\eta O'_\eta(x) \psi_i(x) \psi^*_i(x') O'^*_\eta(x'). \tag{2.8}$$

A basis-independent description of the measurement is an important advantage of the Wigner function formalism introduced in Sec. III.

In Ref. [7] two of us noted that the convolution of the momentum transfer amplitude distribution Eq. (2.5), which we called a quantum momentum transfer, is not in general equivalent to a classical momentum transfer. For a given result ξ, the latter would give rise to a convolution of the momentum probability distribution of the form

$$P_\xi(p) = N_\xi^{-1} \int dp' P_i(p-p') \Omega_\xi(p'), \tag{2.9}$$

where $\Omega_\xi(p)$ is a positive distribution whose integral over all p is equal to N_ξ, the probability of obtaining the result ξ. The initial momentum distribution is $P_i(p) = |\tilde{\psi}_i(p)|^2$. Averaging over all results would give

$$P_f(p) = \int dp' |\tilde{\psi}_i(p-p')|^2 \Omega(p'), \tag{2.10}$$

where $\Omega(p) = \Sigma_\xi \Omega_\xi(p)$. By contrast, the final momentum distribution in the quantum case is

$$P_{\mathrm{f}}(p) = \sum_\xi \left| \int dp' \tilde{\psi}_{\mathrm{i}}(p-p') \tilde{O}_\xi(p') \right|^2 \Big/ 2\pi\hbar, \tag{2.11}$$

which is independent of the basis O_ξ. Expression (2.11) cannot be written in the form of Eq. (2.10) unless there is some basis in which each of the $\tilde{O}_\xi(p)$ is nonzero only at a single point, say p_ξ [7]. In that case, the measurement result ξ tells the observer that the amount of momentum transferred to the particle is exactly p_ξ and

$$\Omega_\xi(p) = |\tilde{O}_\xi(p)|^2 / 2\pi\hbar = N_\xi \delta(p - p_\xi). \tag{2.12}$$

We thus have two reasonable but inequivalent definitions of what constitutes a momentum transfer. Statements made about one type will not in general be true about the other. In the scheme proposed by Scully *et al.*, in contrast to previous well-known examples [1,2], the momentum transfer is quantum, not classical. That is to say, the final momentum distribution cannot be obtained by convolving the initial momentum distribution as in Eq. (2.10). This is what allows the true difference of their scheme, namely, that that there would be negligible disturbance of the momentum of a particle passing through one slit only, as confirmed by their calculations. On the other hand, if the interference fringes were destroyed by classical momentum kicks as in Eq. (2.10), then the single-slit diffraction pattern would necessarily be broadened.

In the double-slit case, the particle's final momentum distribution must be disturbed in some way by the measurement because the interference fringes are destroyed. The momentum separation between node and antinode in the final interference pattern is $\pi\hbar/d$, where d is the slit separation. These fringes cannot disappear without there being some kind of momentum disturbance of order $\hbar/d$, in accord with the uncertainty principle. Storey *et al.* [4–6] have shown that this momentum transfer can be quantified by the momentum transfer amplitudes of Eq. (2.11). Specifically, they have shown that for *any* which-path measurement, at least one $\tilde{O}_\xi(p)$ must be nonzero for some p with $|p| \geq \hbar/d$. In this paper we will recast and strengthen this result using the Wigner function formalism. In this formalism it becomes apparent how a *welcher Weg* measurement scheme, such as that of Scully *et al.*, can transfer momentum of the order $\hbar/d$ in the two-slit case, while having no effect on the momentum distribution in the single-slit case.

III. THE WIGNER FUNCTION

In this section we introduce the Wigner function formalism for describing momentum transfer in *welcher Weg* measurements. This will allow us to place the calculations of Scully *et al.* [3–5] and those of Storey *et al.* [4–6] within a single framework.

A. General formalism

The Wigner function for a wave function $\psi(x)$ is [10]

$$W_\psi(x,p) = \frac{1}{\pi\hbar} \int dy \; B_\psi(x,y) e^{2ipy/\hbar}, \tag{3.1}$$

where

$$B_\psi(x,y) = \psi^*(x+y) \psi(x-y). \tag{3.2}$$

We are interested in the Wigner function of the particle after the measurement. It is

$$W_{\psi_\xi}(x,p)=\frac{1}{\pi\hbar}\int dy\ B_{\psi_\xi}(x,y)e^{2ipy/\hbar}$$
$$=N_\xi^{-1}\frac{1}{\pi\hbar}\int dy\ B_{\psi_i}(x,y)B_{O_\xi}(x,y)e^{2ipy/\hbar}$$
$$=N_\xi^{-1}\frac{1}{\pi\hbar}\int dy\ B_{\psi_i}(x,y)e^{2ipy/\hbar}$$
$$\times\int dy' B_{O_\xi}(x,y')\,\delta(y'-y). \tag{3.3}$$

We now introduce the Fourier transform representation of the Dirac δ function to get

$$W_{\psi_\xi}(x,p)=N_\xi^{-1}\frac{1}{\pi\hbar}\int dy\ B_{\psi_i}(x,y)e^{2ipy/\hbar}$$
$$\times\int dy' B_{O_\xi}(x,y')\frac{1}{\pi\hbar}\int dp' e^{2ip'(y-y')/\hbar}$$
$$=N_\xi^{-1}\int dp'\,\frac{1}{\pi\hbar}\int dy\ B_{\psi_i}(x,y)e^{2i(p-p')y/\hbar}$$
$$\times\frac{1}{\pi\hbar}\int dy' B_{O_\xi}(x,y')e^{2ip'y'/\hbar}$$
$$=N_\xi^{-1}\int dp' W_{\psi_i}(x,p-p')W_{O_\xi}(x,p'). \tag{3.4}$$

That is, the Wigner function transforms exactly as a classical joint probability function if $N_\xi^{-1}W_{O_\xi}(x,p')$ is interpreted as the probability for a particle at position x to receive a momentum transfer of p', given the result ξ. Since N_ξ is the probability of obtaining the result ξ, the Wigner function for the final density matrix, ignoring the measurement result ξ, is

$$W_f(x,p)=\int dp' W_i(x,p-p')W_T(x,p'), \tag{3.5}$$

where $W_i(x,p)=W_{\psi_i}(x,p)$ and

$$W_T(x,p)=\sum_\xi W_{O_\xi}(x,p). \tag{3.6}$$

Like $\rho_f(x,x')$ in Eq. (2.7), the total momentum transfer function $W_T(x,p)$ is independent of the basis O_ξ, which is one of the advantages of the formalism. (Another advantage is that the formalism can be generalized to allow measurements that do not preserve purity, although we will not consider such measurements in this paper.)

For the case of classical momentum kicks (2.12), the momentum transfer function can be worked out as follows. First we note that

$$O_\xi(x)=\sqrt{N_\xi}\exp(ip_\xi x/\hbar), \tag{3.7}$$

so that

$$B_{O_\xi}(x,y)=N_\xi\exp(-2ip_\xi y/\hbar), \tag{3.8}$$

which gives

$$W_T(x,p)=\sum_\xi N_\xi\delta(p-p_\xi)=\Omega(p). \tag{3.9}$$

This is a weighted sum of the classical momentum kicks p_ξ associated with the measurement outcomes ξ and is independent of x. Note that $\Sigma_\xi N_\xi=1$, which follows from Eq. (2.2). The Wigner function (3.9) is non-negative everywhere. It has an obvious interpretation as a classical momentum kick probability distribution function. However, in general the momentum transfer Wigner function (3.6) need not be positive semidefinite.

Although it is not necessarily positive semidefinite, the transfer Wigner function $W_T(x,p)$ is always normalized in p, in the sense that

$$\int dp\ W_T(x,p)=1 \tag{3.10}$$

for all x. This is a consequence of the completeness condition (2.2). In fact, it is also possible to prove a more general result, namely, that the characteristic function

$$\Phi_T(q|x)=\int dp\ W_T(x,p)\exp(ipq/\hbar) \tag{3.11}$$

satisfies

$$|\Phi(q|x)|\leqslant 1, \tag{3.12}$$

just as it would if $W_T(x,p)$ were a true probability distribution in p. This can be proved as

$$\Phi(q|x)=\int dp\ e^{ipq/\hbar}\frac{1}{2\hbar}\sum_\xi\int dy\ B_{O_\xi}(x,y)e^{i2py/\hbar}$$
$$=\sum_\xi\int dy\ \delta(y+q/2)O_\xi^*(x+y)O_\xi(x-y)$$
$$=\sum_\xi O_\xi^*(x-q/2)O_\xi(x+q/2). \tag{3.13}$$

Finally, it follows that

$$|\Phi(q|x)|\leqslant\sum_\xi |O_\xi^*(x-q/2)||O_\xi(x+q/2)|$$
$$\leqslant\tfrac{1}{2}\sum_\xi |O_\xi(x-q/2)|^2+|O_\xi(x+q/2)|^2, \tag{3.14}$$

where the last line is obtained by using the fact that $(|A|-|B|)^2\geqslant 0$. From the completeness condition (2.2), we thus obtain the desired result (3.12).

B. Wigner functions in double-slit experiments

1. $W_i(x,p)$

In a double-slit experiment $W_i(x,p)$ has peaks at $x=\pm d/2$ (the slit positions) and also a part at $x=0$ that is oscillatory in p. For zero slit width

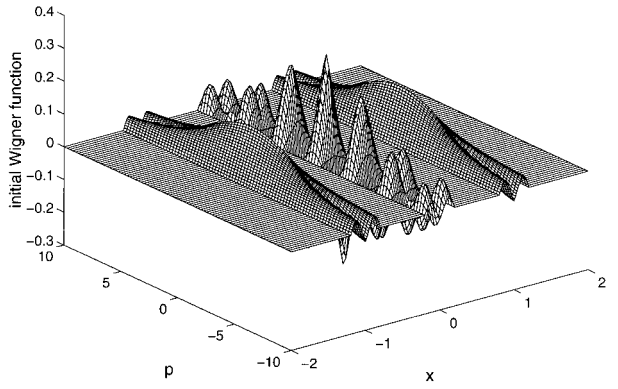

FIG. 1. Plot of the initial Wigner function $W_i(x,p)$ for a double-slit experiment, with $d=2$ and $a=0.2d=0.4$. The slits produce wave packets centered at $x=\pm 1$ with a full width of 0.4. Momentum is scaled by setting $\hbar=1$.

$$W_i(x,p)\propto\frac{1}{2}[\,\delta(x-d/2)+\delta(x+d/2)\,]+\delta(x)\cos\frac{pd}{\hbar}. \tag{3.15}$$

This will be a valid idealization provided that the slit width a is much less than the scale of variation of $W_T(x,p)$ in x around $x=\pm d/2$ and $x=0$. This requirement is satisfied for most of the cases we examine as long as $a\ll d$. In Fig. 1 we show this initial Wigner function for rectangular slits with width $a=0.2d$. The oscillations in Eq. (3.15) at $x=0$ average to zero when integrated over p so that the probability distribution for the particle position is

$$P_i(x)=\int dp\ W_i(x,p)=\tfrac{1}{2}[\,\delta(x-d/2)+\delta(x+d/2)\,]. \tag{3.16}$$

When we integrate over x to find the momentum distribution, it is the oscillations that produce the interference pattern, highlighting the nonlocal nature of the initial superposition:

$$P_i(p)=\int dx\ W_i(x,p)\ \propto\ 1+\cos\frac{pd}{\hbar}. \tag{3.17}$$

In the far field (a long way past the slits), this interference in momentum becomes the observed interference pattern in position.

2. $P_{\text{nonlocal}}(p)$

The interference fringes in momentum are destroyed in *welcher Weg* measurements. As noted above, these fringes are present due to the coherence between the parts of the wave function at $x=\pm d/2$ and appear as oscillations in the Wigner function at $x=0$. This means that to destroy interference the oscillations in the initial Wigner function in the region of $x=0$ must be effaced. In a *welcher Weg* measurement, this happens through convolution with the transfer function in that region. Provided that $W_T(x,p)$ varies little as a function of x over a region of width a around $x=0$, we can take the destruction to be due to $W_T(x,p)$ at $x=0$. That is, in the Wigner function formalism, the pseudoprobability distribution for the momentum transfers that destroy the interference is

$$P_{\text{nonlocal}}(p)=W_T(0,p). \tag{3.18}$$

We label this $P_{\text{nonlocal}}(p)$ because it is the distribution function for momentum transfers at the point midway between the slits, where the probability for finding the particle is zero. Although $P_{\text{nonlocal}}(p)$ is normalized, it is not necessarily positive definite.

Because it is the momentum transfers described by $P_{\text{nonlocal}}(p)$ that are responsible for destroying the interference fringes, the visibility can be found from $P_{\text{nonlocal}}(p)$ alone. After passing through the *welcher Weg* detectors, the Wigner function at $x=0$ is given by

$$\begin{aligned}W_f(0,p)&=\int dp'\,W_T(0,p')\cos\frac{(p-p')d}{\hbar}\\&=\mathrm{Re}[\,e^{ipd/\hbar}\mathcal{V}^*],\end{aligned} \tag{3.19}$$

where we have defined a complex visibility

$$\mathcal{V}=\int dp\ P_{\text{nonlocal}}(p)e^{ipd/\hbar}. \tag{3.20}$$

We call this the complex visibility because its modulus gives the fringe visibility and its phase gives the phase of the fringes. This can be seen in the final momentum distribution, which, from Eq. (3.19), is

$$P_f(p)=\int dx\ W_f(x,p)\propto 1+V\cos\left(\frac{pd}{\hbar}-\arg\mathcal{V}\right), \tag{3.21}$$

where we are using $V=|\mathcal{V}|$ for the (usual) visibility. In the absence of any *welcher Weg* measurement the fringe visibility is unity. Any measurement that gives some information about which path the particle took will reduce the visibility to less than unity. A perfect *welcher Weg* measurement, one that determines with certainty which way the particle went, will reduce the visibility to zero.

3. $P_{\text{local}}(p)$

The fact that $P_{\text{nonlocal}}(p)$ determines the visibility runs counter to classical intuition. Classically, one would expect the particle to be affected only by the momentum transfers at the positions of the slits (which are the only places where the probability to find the particle is nonzero). Since $W_T(x,p)$ plays the role of the probability distribution for a particle at position x to receive a momentum transfer p, classically one would expect the distribution of momentum kicks given to the particle to be $W_T(x,p)$ averaged over the possible positions of the particle distributed according to $P_i(x)$. That is to say, classically one would expect the relevant kick distribution to be

$$P_{\text{local}}(p)=\int dx\ W_T(x,p)P_i(x). \tag{3.22}$$

For the case in question where the particle is localized at the two slits, the pseudoprobability distribution function for these local momentum transfers is

$$P_{\rm local}(p)=\frac{1}{2}[W_T(d/2,p)+W_T(-d/2,p)]. \quad (3.23)$$

Although $P_{\rm local}(p)$ plays no role in the destruction of interference between the two paths, it does determine the diffraction pattern of a particle that is in a classical mixture of being at the two slits. Provided that the momentum transfer Wigner function is the same at both slits (which we will assume below), this is the same as the diffraction pattern from a single slit. The final momentum distribution for an arbitrary initial state in a *welcher Weg* scheme is

$$P_f(p)=\int dx\ W_f(x,p)dx$$

$$=\int dx\int dp' W_i(x,p-p')W_T(x,p'). \quad (3.24)$$

If the particle is in a mixture then there are no oscillations in $W_i(x,p)$ at $x=0$ and indeed $W_i(x,p)$ is nonzero only for $x\approx\pm d/2$. Thus we can replace $W_T(x,p)$ by $W_T(\pm d/2,p)=P_{\rm local}(p)$, giving

$$P_f(p)=\int dx\int dp' W_i(x,p-p')P_{\rm local}(p') \quad (3.25)$$

$$=\int dp' P_i(p-p')P_{\rm local}(p'). \quad (3.26)$$

It follows from the properties of convolutions that the moments of $P_f(p)$ in this case are determined by $P_{\rm local}(p)$. For example, $\overline{p_f}=\overline{p_i}+\overline{p_{\rm local}}$, where $\overline{p_f}=\int dp P_f(p)p$, *etc.*, and also

$$\underset{f}{\rm Var}(p)=\underset{i}{\rm Var}(p)+\underset{\rm local}{\rm Var}(p), \quad (3.27)$$

where ${\rm Var}_f(p)=\int dp\ P_f(p)(p-\overline{p_f})^2$, etc.

In addition to determining the diffraction pattern of a single slit (or a mixture), $P_{\rm local}(p)$ also determines the broadening of the diffraction envelope under which the interference fringes lie in the double-slit case. This can be seen as follows. Provided the slit width a is much smaller than the slit separation d, the moments of the final momentum distribution in the double-slit case are determined solely by the non-oscillatory parts of the Wigner function around $x=\pm d/2$. The contribution to the total momentum distribution from the oscillatory part of the initial Wigner function near $x=0$ for slits of width a centered at $x=\pm d/2$ can be shown to be

$$\frac{a}{\pi\hbar}\left(\frac{\sin ap/2\hbar}{ap/2\hbar}\right)^2\left(\cos^2\frac{pd}{2\hbar}-\frac{1}{2}\right). \quad (3.28)$$

All of the moments of this function are zero in a distributional sense [11]. This is necessarily so because the moments of this part of the Wigner function are weighted by the norm of this part. This norm [the integral of $W_i(x,p)$ over all p and x near 0] is strictly zero because it is equal to the probability of finding the particle there. After a *welcher Weg* measurement this norm is still strictly zero, so the moments of the final momentum distribution $P_f(p)$ are determined by the parts of the Wigner function near $x=\pm d/2$. As shown above, these parts are broadened by the action of $P_{\rm local}(p)$. Therefore, the relationship (3.27) showing that the increment in the momentum variance is equal to the variance of $P_{\rm local}(p)$ applies to the double-slit as well as to the single-slit case.

C. Minimum disturbance to destroy interference

1. Arbitrary momentum transfers

Storey *et al.* [6] have shown that in an arbitrary *welcher Weg* measurement that reduces the fringe visibility to V, at least one momentum transfer amplitude distribution $\widetilde{O}_\xi(p)$ must be nonzero for some $p\geqslant(1-V)\hbar/d$. In terms of the Wigner function, this is equivalent to the statement that $W_T(x,p)$ must be nonzero for some x and some $p\geqslant(1-V)\hbar/d$. We have shown above that the fringe visibility is determined solely by $P_{\rm nonlocal}(p)$ as in Eq. (3.20). This will allow us to derive a stronger theorem concerning momentum transfer, in the sense that we need consider only $W_T(x,p)$ at $x=0$, not for any possible x.

In order to quantify the nonlocal momentum transfer we introduce the function

$$A(x)=\int dp\ P_{\rm nonlocal}(p)e^{ipx/\hbar}, \quad (3.29)$$

so that by Eq. (3.20), $\mathcal{V}=A(d)$. We have, by normalization (3.10),

$$A(0)=\int dp\ P_{\rm nonlocal}(p)=1 \quad (3.30)$$

and also that for all x, $|A(x)|\leqslant 1$, which follows from Eq. (3.12) since $A(x)=\Phi(x|0)$. In Appendix A we show, using a theorem due to Boas [12], that any well-behaved function $A(x)$ satisfying the three conditions

$$A(0)=1, \quad A(d)=\mathcal{V}, \quad |A(x)|\leqslant 1 \quad \forall x \quad (3.31)$$

has a Fourier transform

$$\widetilde{A}(k)=\frac{1}{\sqrt{2\pi}}\int dx\ e^{-ikx}A(x), \quad (3.32)$$

which cannot have support only on a closed interval $[-K,K]$ for any $K<\arccos(|\mathcal{V}|)/d$. That is to say,

$$\widetilde{A}(k)\neq 0 \quad \text{for some } k, \quad |k|\geqslant\arccos(V)/d, \quad (3.33)$$

where $V=|\mathcal{V}|$ as above. Given the relation (3.29) between $A(x)$ and $P_{\rm nonlocal}(p)$, we can thus say that

$$P_{\rm nonlocal}(p)\neq 0 \quad \text{for some } p, \quad |p|\geqslant p_m, \quad (3.34)$$

where we have defined

$$p_m=\arccos(V)\hbar/d. \quad (3.35)$$

This expression for p_m is an improvement over the previous lower bound of $(1-V)\hbar/d$ derived by Storey *et al.* [6] using an earlier theorem due to Bernstein [13]. Our result gives a much larger lower bound on the momentum transfer necessary to reduce the visibility slightly below unity. This is not surprising given the durability of interference fringes in the face of imperfect *welcher Weg* information, pointed out by Wooters and Zurek [14]. In the other limit, if the visibility is reduced to zero, we have

$$p_m=\frac{\pi\hbar}{2d} \tag{3.36}$$

compared with $\hbar/d$ derived by Storey *et al.* Moreover, our lower bound is the greatest lower bound for the case $\mathcal{V}=V$. This is the case where the measurement decreases the visibility of the fringes but does not alter their positions (which would be a deterministic effect rather than a random momentum disturbance). The function

$$A(x)=\cos[\arccos(V)x/d] \tag{3.37}$$

satisfies the three requirements (3.31) for $\mathcal{V}=V$, and has a Fourier transform that is zero for $k>\arccos(V)/d$. We shall show in Sec. IV C that there is a physically realizable perfect $(V=0)$ *welcher Weg* experiment that has a momentum transfer of exactly $\pi\hbar/2d$ in magnitude.

2. Classical momentum kicks

In the case of classical momentum kicks, we can extend the result we have just derived as follows. Not only must there be some transfer of momentum at least equal to p_m, but the root-mean-squared nonlocal momentum transfer must be at least equal to this amount. This is because any true probability distribution $P(p)$ that obeys

$$\int dp\ P(p)e^{ipd/\hbar}=\mathcal{V} \tag{3.38}$$

has a standard deviation satisfying

$$\sigma(p)\geqslant\arccos(V)\hbar/d. \tag{3.39}$$

The proof of this theorem is in Appendix B. As shown there, any scheme that attains this minimum standard deviation will also have a momentum disturbance precisely equal to p_m [15].

For the case where the visibility is zero, we can recast the inequality (3.39) in a form resembling the Heisenberg uncertainty relation:

$$\sigma(p)\sigma(x)\geqslant\frac{\pi\hbar}{4}, \tag{3.40}$$

where $\sigma(x)=d/2$ is the standard deviation in the particle's position. However, the interpretations of the terms on the left-hand side of this equation are quite different from those in the uncertainty relations derived from the noncommutation of operators [16]. Specifically, $\sigma(p)$ is the standard deviation of the distribution of momentum kicks given to the particle rather than the standard deviation of the distribution of the particle's momentum (either before or after the measurement). Hence the fact that the there is a numerical factor of $\pi/4$ rather than 1/2 on the right-hand side is no cause for surprise. As noted above, the relation (3.40) applies only for classical momentum kicks for which $P_{\text{nonlocal}}(p)=W_T(x,p)$ is a true probability distribution for momentum kicks. For quantum *welcher Weg* schemes, $P_{\text{nonlocal}}(p)$ cannot be interpreted this way and is not necessarily positive semidefinite. In those cases the standard deviation may even be zero, as we will see. Whereas the local momentum disturbance is usefully characterized by the variance of $P_{\text{local}}(p)$, the variance of $P_{\text{nonlocal}}(p)$ is not a relevant quantity. In general we can say only that $P_{\text{nonlocal}}(p)$ must be nonzero for some p satisfying $pd\geqslant\pi\hbar/2$.

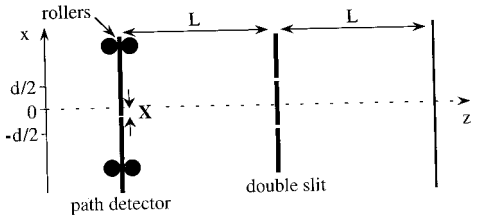

FIG. 2. Diagram of the Einstein recoiling slit *welcher Weg gedankenexperiment*. The recoiling slit is the path detector and has position X, while the particle has position x.

In their papers [3–5], Scully *et al.* quantified momentum transfer by considering the effect of their *welcher Weg* scheme on the momentum distribution of a particle localized at a single slit. As shown in Sec. III B 3, this probes the moments of $P_{\text{local}}(p)$. Scully *et al.* demonstrated that the disturbance to such a particle can be negligibly small, even though the same device can destroy the interference fringes in the double-slit case. This is possible because in the case of a quantum momentum transfer (such as in the scheme of Scully *et al.*), there can be a nonlocal momentum disturbance through $P_{\text{nonlocal}}(p)$ despite there being no broadening of the diffraction envelope by $P_{\text{local}}(p)$. This is in contrast to classical momentum kicks for which $W_T(x,p)$ is everywhere positive and independent of x. Then the final momentum distribution is a convolution of the initial momentum distribution with a positive distribution of momentum kicks [see Eq. (2.10)] that is equal to $W_T(x,p)$. As shown above [Eq. (3.40)], the standard deviation of such a classical distribution is necessarily greater than or equal to $\pi\hbar/2d$ if the interference fringes are to be effaced. That is to say, for classical *welcher Weg* schemes, the destruction of interference is always accompanied by broadening of the diffraction envelope in line with the uncertainty principle.

IV. EXAMPLES OF CLASSICAL MOMENTUM KICKS

A. Einstein's recoiling slit

The oldest example of a *welcher Weg* measurement is Einstein's recoiling slit. The slit in question is positioned such that the particles must pass through it prior to passing through the double slits, as shown in Fig. 2. The recoiling slit is so named because the screen in which it is situated is free to move on rollers. In this manner, the momentum kick given to the slit as the particle heads for either the upper or lower slit in the second screen should enable one to determine which of these slits it goes through. Measuring the recoiling

slit momentum will only distinguish the path of the particle if σ, the uncertainty in the position of the single (recoiling) slit, is very much less than d, the separation of the double slits. This was shown quantitatively by Tan and Walls [17]. Einstein thought that this scheme would work as a *welcher Weg* measurement without destroying the interference pattern (and hence that quantum mechanics was incomplete), but Bohr proved him wrong by arguing that for consistency the recoiling screen must also be treated as a quantum-mechanical object [1] so that the uncertainty σ in the position of the recoiling slit is inversely related to the uncertainty in its momentum. Let the wave function of the recoiling screen be

$$\phi(X)=(2\pi\sigma^2)^{-1/4}\exp[-(X/\sigma)^2/4], \tag{4.1}$$

where X is the position of the recoiling slit. The recoiling screen will be assumed to have infinite mass so that the transfer of momentum to it does not alter its position probability distribution

$$P_E(X)=(2\pi\sigma^2)^{-1/2}\exp[-(X/\sigma)^2/2]. \tag{4.2}$$

Let the horizontal distance between the first and the second screen be $L\gg\sigma,d$, so that we may use the paraxial approximation. Then the joint wave function for the position of the recoiling slit X and the displacement of the particle at the second slit is

$$\Psi(x,X)\propto\phi(X)\exp[ik(x-X)^2/2L], \tag{4.3}$$

where k is the longitudinal wave number for the particle (assumed constant). Alternatively, we can write

$$\Psi(x,X)\propto\exp[ikx^2/2L]\exp[ikX^2/2L]O_X(x). \tag{4.4}$$

The first factor is the phase front of a circular wave in the paraxial approximation, which is present regardless of the position of the recoiling slit. The second factor involves only the slit position and is of unit magnitude, so it is irrelevant to the particle. The final factor is the important one:

$$O_X(x)=\sqrt{P_E(X)}\exp[-ikXx/L]. \tag{4.5}$$

This is the operator that acts on the particle's wave function given that a particular position X of the recoiling slit has been measured.

This result shows that if we measure the *position* X of the recoiling slit after the particle has passed through, we give the particle a classical momentum kick of amplitude $p=-\hbar kX/L$ rather than finding out which way it went (as we would from a measurement of the slit's *momentum*). As pointed out by Wooters and Zurek [14], the subensemble of atoms conditioned on a particular result X will have perfect fringe visibility even though the visibility of the fringes of the total ensemble is arbitrarily small. This effect (in another system) was subsequently called the *quantum eraser* by Scully and Drühl [18]. The applicability of the quantum eraser concept to all *welcher Weg* schemes was discussed by Bhandari [19] and by Tan and Walls [17].

Given the probability density for measuring the recoiling slit position (4.2), the probability density for delivering a momentum kick to the particle is $P_E(Lp/\hbar k)L/\hbar k$. That is to say, the momentum transfer Wigner function is

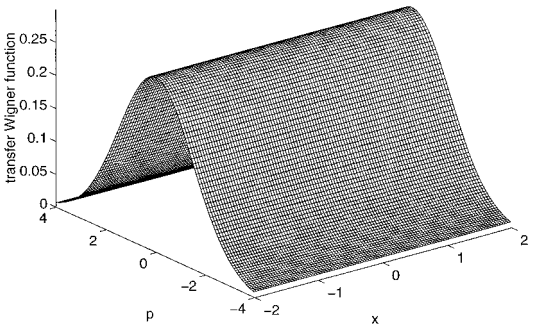

FIG. 3. Plot of the momentum transfer Wigner function $W_T(x,p)$ for the Einstein recoiling slit. The parameters chosen give a fringe visibility of 1%. As usual, we have $d=2$ and $\hbar=1$.

$$W_T(x,p)=\frac{L}{\hbar k\sigma\sqrt{2\pi}}\exp\left[-\frac{1}{2}\left(\frac{pL}{\hbar k\sigma}\right)^2\right] \tag{4.6}$$

and $P_{\text{nonlocal}}(p)=P_{\text{local}}(p)=W_T(x,p)$. The standard deviation of the momentum transfer in this case is $\sigma(p)=\hbar k\sigma/L$. As shown in Ref. [17], the effect of these momentum kicks is to reduce the visibility of the interference fringes by a factor

$$V=\exp[-\tfrac{1}{2}(k\sigma d/L)^2]. \tag{4.7}$$

Thus the initial Gaussian shape of the wave packet for the recoiling slit means that the fringe visibility can never be reduced to zero. However, the visibility is reduced to about 1% for $kd\sigma/L=3$, that is, for $\sigma(p)=3\hbar/d$. This is well above the lower bound on the momentum transfer p_m required for destruction of interference (3.36). In Fig. 3 we plot the momentum transfer Wigner function for this case.

B. Feynman's light microscope

Another familiar *welcher Weg* scheme, also considered by Tan and Walls [17], is Feynman's light microscope. Here we follow their presentation and take the particle passing through the double slits to be an atom. Immediately after this passage the atom is illuminated by a photon of momentum K traveling in the x direction, as shown in Fig. 4. This photon is assumed to be scattered by the atom in a random direction, giving a momentum kick to the atom. As shown in [17], the probability distribution for the x component of the momentum of the scattered photon (be it circularly or linearly polarized) is

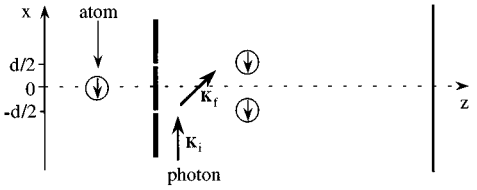

FIG. 4. Diagram of the Feynman light microscope *welcher Weg* scheme. The atom scatters a photon in a random direction.

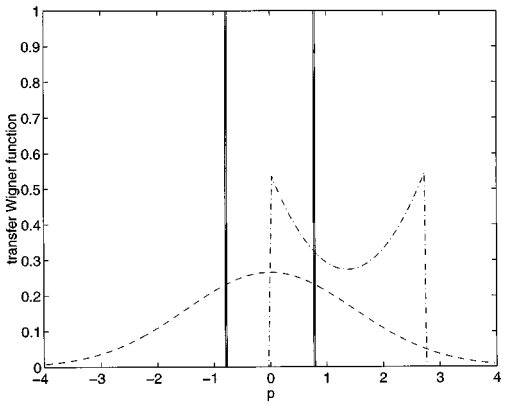

FIG. 5. Plot of the momentum kick probability distributions for the three classical *welcher Weg* schemes considered. They are the Einstein recoiling slit from Sec. II A (dashed line), the Feynman light microscope from Sec. IV B (dash-dotted line), and the minimally disturbing atom optics scheme from Sec. IV C (solid line).

$$P_F(k_x)=\frac{1}{K}B(k_x/K), \tag{4.8}$$

where

$$B(u)=\tfrac{3}{8}(1+u^2)H(1-u^2) \tag{4.9}$$

and H is the Heaviside function, which is one for a positive argument and zero for a negative argument. In this case, the total momentum kick is offset from zero due to the momentum absorbed from the incoming photon:

$$W_T(x,p)=\frac{1}{\hbar K}B\left(\frac{p}{\hbar K}-1\right). \tag{4.10}$$

Tan and Walls show that the effect of the momentum kicks is to reduce the complex visibility to

$$\mathcal{V}=\frac{3}{2}e^{iKd}\left(\frac{\cos Kd}{(Kd)^2}+\frac{\sin Kd}{Kd}-\frac{\sin Kd}{(Kd)^3}\right). \tag{4.11}$$

This is an oscillatory function of Kd and tends to zero as $Kd\to\infty$. Its zeros cannot be found analytically, but numerically the first zero is found at $Kd\approx 2.74$. Choosing K to have this value will give the minimum momentum disturbance compatible with complete destruction of the interference pattern. In this case, a perfectly accurate *welcher Weg* measurement can in principle be made by detecting the outgoing photon to be in one of two possible modes, corresponding to the scattering center being at the upper or lower slit [17]. In Fig. 5 we have plotted the transfer Wigner function for $K=2.74/d$. The standard deviation for the momentum transfer in this case is

$$\sigma(p)\approx\frac{2.74\sqrt{2}\,\hbar}{\sqrt{5}\,d}\approx 1.73\frac{\hbar}{d}, \tag{4.12}$$

which is greater than $p_m\approx 1.57\hbar/d$.

Recently, preliminary experiments have been made with the ultimate goal of creating a Feynman light microscope [20]. Pfau *et al.* [20] and Clauser and Li [21] have shown the effect of a single spontaneous emission on atomic diffraction and interference patterns, respectively. Very recently, Chapman *et al.* [22] have done likewise using a Mach-Zehnder atomic interferometer in which the fringes were observed as a function of the relative positions of the gratings. A photon of momentum $\hbar K$ was scattered off the atom at a longitudinal position where the distance between the centers of the two beams was d. The fringe visibility depends on Kd in the same way as in Eq. (4.11), and this was verified in the experiment by varying d. In addition, the lost visibility was partially regained, in a manner resembling a quantum eraser, by conditioning the atoms on their coarse-grained position at the third grating. However, for this technique to work, the beam width has to be much larger than d, so that detection of the emitted photon could not distinguish between the two paths taken by the atom even in principle [23].

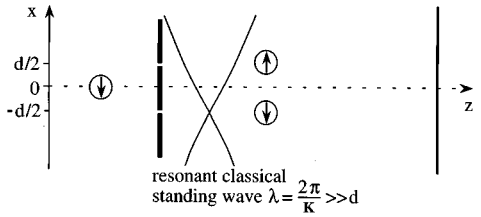

FIG. 6. Diagram of the minimally disturbing *welcher Weg* scheme. The particle is an atom with two internal states that act as the *welcher Weg* detector. It is initially in the ground state (down arrow), but becomes excited (up arrow) if it passes through the upper slit.

C. A minimally disturbing atom optics scheme

As the final example of a classical *welcher Weg* measurement we here propose a scheme that has the interesting feature of attaining the lower bound on the momentum transfer derived in Sec. III C. The two slits are immediately followed by a classical standing-wave light field with wavelength $2\pi/K\gg d$. The particle is again taken to be a two-level atom that is resonant with the light field. In the absence of spontaneous emission [24], the Hamiltonian for the interaction is

$$H=\hbar\Omega\sigma_1\sin[K(x-x_0)]. \tag{4.13}$$

Here Ω is the Rabi frequency and $\sigma_1=|g\rangle\langle e|+|e\rangle\langle g|$, where $|e\rangle$ and $|g\rangle$ are the excited and ground states of the atom, respectively. In this case it is the internal states of the atom that act as the measuring apparatus.

We now choose $x_0=-d/2$ so that the lower slit is at a node of the field, as shown in Fig. 6. Since $Kd\gg 1$ we can locally approximate the Hamiltonian as

$$H=\hbar\Omega K\sigma_1(x+d/2). \tag{4.14}$$

Let the atom be prepared in the ground state and let the interaction time be $t=\pi/2\Omega Kd$, so that at the upper slit the atom experiences a π pulse. Then the final state of the atom is

$$|\Psi\rangle=\int dx\,\exp\left[-i\left(\frac{\pi x}{2d}+\frac{\pi}{4}\right)\sigma_1\right]\psi(x)|x\rangle|g\rangle. \tag{4.15}$$

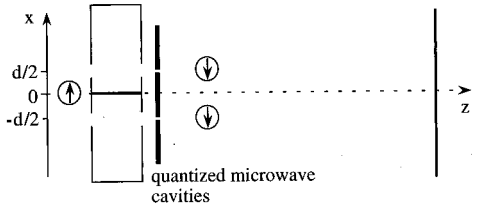

FIG. 7. Diagram of the Scully-Englert-Walther *welcher Weg* scheme. The microwave cavities are initially empty and act as the *welcher Weg* detectors as the atom deexcites, depositing a photon.

A measurement of the internal state of the atom in the $\sigma_3=|e\rangle\langle e|-|g\rangle\langle g|$ basis determines which way the atom went. The result $\xi(\sigma_3)=-1$ indicates that the atom's internal state has not changed from the initial $|g\rangle$, so its path must have been via the lower slit and through the node at $x=-d/2$. The result $\xi(\sigma_3)=1$ indicates that its path was via the upper slit at $x=d/2$, where the atom becomes excited.

For this system the complementary observable (which erases the *welcher Weg* information) is σ_1. In the σ_1 basis the two results $\xi(\sigma_1)=\pm 1$ yield the measurement functions

$$O_{\pm}(x)=\frac{1}{\sqrt{2}}\exp\left(\mp i\frac{\pi x}{2d}\right), \tag{4.16}$$

where a global (i.e., independent of x) phase factor has been ignored, in the same manner as in Eq. (4.5). The functions $O_{\pm}(x)$ give a momentum kick to the atom of $p_{\pm}=\mp\hbar\pi/2d$, respectively. The momentum transfer Wigner function is

$$W_T(x,p)=\frac{1}{2}\left[\delta\left(p-\frac{\hbar\pi}{2d}\right)+\delta\left(p+\frac{\hbar\pi}{2d}\right)\right], \tag{4.17}$$

which is positive semidefinite. Its destruction of the interference pattern can easily be understood because each momentum kick shifts the entire fringe pattern by $\pm\hbar\pi/2d$, which is precisely the amount required to move the nodes of one shifted pattern onto the antinodes of the other shifted pattern. This scheme provides a physical mechanism for a *welcher Weg* measurement in which there is no momentum disturbance greater than the requisite minimum of $p_m=\pi\hbar/2d$. It also achieves the minimum classical root-mean-squared momentum transfer, given by Eq. (3.39).

V. EXAMPLES OF QUANTUM MOMENTUM TRANSFERS

A. The Scully-Englert-Walther scheme

We now consider the experiment proposed by Scully *et al.* [3], shown in Fig. 7. This involves two initially empty microwave cavities with flat mode functions in the x direction. The atom starts in an excited Rydberg state and the time of passage through the cavities is chosen so that it undergoes exactly one-half Rabi cycle, deexciting to another Rydberg state and emitting a microwave photon. The presence of this photon in either the upper or lower cavity reveals the path of the atom. As Scully *et al.* have shown, the flatness of the mode functions means that this emission causes no local momentum kick to the atom.

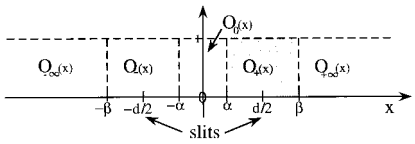

FIG. 8. Diagram of the five regions involved in our model of the Scully-Englert-Walther *welcher Weg* scheme.

As shown in Fig. 7, atoms are allowed to enter the cavity only through holes in the cavity walls in the region of $x=\pm d/2$. In the experiment considered by Scully *et al.*, all atoms would pass through these holes because the atoms have already been collimated. However, in order to calculate $W_T(x,p)$ we must have some model for what would happen to atoms for all possible x. For this reason, we divide space in the x direction into five regions, as shown in Fig. 8. Two of these correspond to the regions in which atoms pass through the cavities and are thereby distinguished. Under ideal conditions, this measurement can be treated as a projective measurement on those two regions, with an error of order 10^{-25} as shown by Scully *et al.* in Ref. [4]. That is, the measurement functions will be the characteristic functions of the regions

$$O_{+}(x)=\mathcal{X}_{(\alpha,\beta)}(x), \tag{5.1}$$

$$O_{-}(x)=\mathcal{X}_{(-\beta,-\alpha)}(x), \tag{5.2}$$

where

$$\mathcal{X}_{(a,b)}(x)=\begin{cases}1 & \text{for} \quad a<x<b\\ 0 & \text{for} \quad x<a \quad \text{or} \quad b<x.\end{cases} \tag{5.3}$$

Atoms impinging upon the other regions would be absorbed. This could be modeled by transferring an infinite momentum kick to those atoms so that they would be expelled from the paraxial region and therefore not contribute to the final pattern. However, in this experiment the initial state is such that no atoms will impinge upon these three other regions, so we can model them as three independent transmitting regions without affecting the calculated pattern. Since an absorber would localize the particle on an atomic scale, it would disturb the particle's transverse momentum much more than a transmitter would. Thus we can be confident that in replacing absorbing regions (upon which atoms never fall) by transmitting regions, we are if anything underestimating any possible nonlocal momentum transfer. Therefore, we complete the description of the measurement with the three measurement functions

$$O_{+\infty}(x)=\mathcal{X}_{(\beta,\infty)}(x), \tag{5.4}$$

$$O_{0}(x)=\mathcal{X}_{(-\alpha,\alpha)}(x), \tag{5.5}$$

$$O_{-\infty}(x)=\mathcal{X}_{(-\infty,-\beta)}(x). \tag{5.6}$$

The Wigner function for $O_{+}(x)$ is

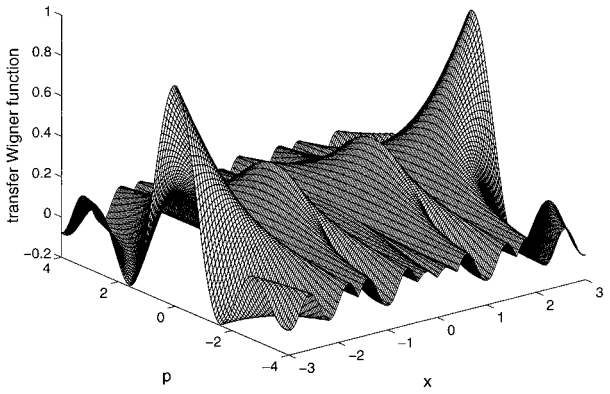

FIG. 9. Plot of $W_T(x,p)$ for the Scully-Englert-Walther *welcher Weg* scheme for $\alpha=d/5=0.4$ and $\beta=4d/5=1.6$.

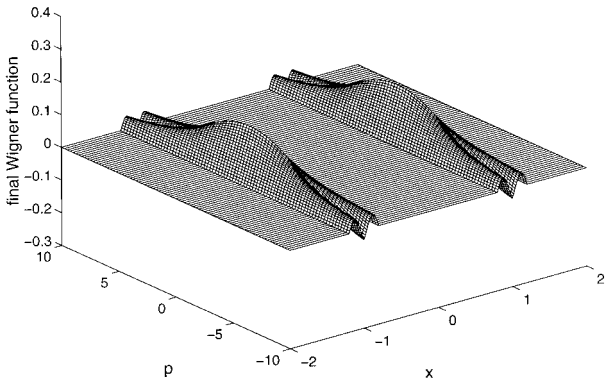

FIG. 10. Plot of $W_f(x,p)$ for the Scully-Englert-Walther *welcher Weg* scheme, with $W_T(x,p)$ as in Fig. 9 and the initial Wigner function as plotted in Fig. 1. As usual, we have $d=2$ and $\hbar=1$.

$$W_{O_+}(x,p)=\frac{1}{\pi\hbar}\int dy\ \mathcal{X}_{(\alpha,\beta)}(x+y)\mathcal{X}_{(\alpha,\beta)}(x-y)e^{2ipy/\hbar}$$
$$=\frac{1}{\pi\hbar}\mathcal{X}_{(\alpha,\alpha/2+\beta/2)}\int_{\alpha-x}^{x-\alpha}dy\ e^{2ipy/\hbar}$$
$$+\frac{1}{\pi\hbar}\mathcal{X}_{(\alpha/2+\beta/2,\beta)}\int_{x-\beta}^{\beta-x}dy\ e^{2ipy/\hbar}$$
$$=\frac{1}{\pi p}\mathcal{X}_{(\alpha,\alpha/2+\beta/2)}\sin\frac{2p(x-\alpha)}{\hbar}$$
$$+\frac{1}{\pi p}\mathcal{X}_{(\alpha/2+\beta/2,\beta)}\sin\frac{2p(\beta-x)}{\hbar}. \qquad (5.7)$$

The other Wigner functions may be evaluated similarly and are all nonzero only within their respective regions in the x direction, going to zero at the boundaries between the regions. The total transfer Wigner function is plotted in Fig. 9. We have chosen $\alpha=(1/5)d$ and $\beta=(4/5)d$, which are the values suggested by Scully *et al.* in Ref. [4]. As shown in Sec. III A, the Wigner function for the final density matrix $W_f(x,p)$ is obtained by convolving the transfer Wigner function $W_T(x,p)$ with the initial Wigner function $W_i(x,p)$ [Eq. (3.5)]. For the initial state shown in Fig. 1, the final Wigner function after the measurement of Scully *et al.* is plotted in Fig. 10. As expected, given that a *welcher Weg* measurement destroys the interference pattern, the measurement completely effaces the oscillations between the slits in the initial Wigner function.

From Fig. 9 it can be seen that $W_T(x,p)$ is not positive semidefinite, demonstrating the quantum nature of this measurement, as compared to the classical cases above. The nonlocal momentum transfer distribution is

$$P_{\text{nonlocal}}(p)=\frac{1}{\pi p}\sin\frac{2p\alpha}{\hbar}. \qquad (5.8)$$

This extends over all p and thus satisfies our theorem on the momentum transfer required to destroy interference fringes (3.34). Furthermore, it has a characteristic width of order $\hbar/2\alpha$ (although its standard deviation is zero in a distributional sense [11]). In order to distinguish between atoms at the two positions $x=\pm d/2$, α must be less than $d/2$. Hence the characteristic width of $P_{\text{nonlocal}}(p)$ must be at least of order $\hbar/d$, as expected from the uncertainty principle. The fringe visibility can be calculated to be

$$\mathcal{V}=\int dp\, P_{\text{nonlocal}}(p)e^{ipd/\hbar}=H(\alpha-d/2), \qquad (5.9)$$

where $H(\alpha-d/2)$ is the Heaviside function, which is zero for $\alpha<d/2$.

The local momentum transfer is described by

$$P_{\text{local}}(p)=\frac{1}{\pi p}\sin\frac{3pd}{5\hbar}, \qquad (5.10)$$

where (as in Fig. 9) we are using the parameters $\alpha=(1/5)d$ and $\beta=(4/5)d$ suggested by Scully *et al.* This also has a characteristic width of order $\hbar/d$, which seems to suggest that a particle passing through one slit would receive some sort of momentum disturbance in accordance with Heisenberg's uncertainty principle. However, this appearance is illusory, as can be verified from the final Wigner function plotted in Fig. 10. As shown in Sec. III B 3, the relevant quantities that characterize the amount of momentum transferred by $P_{\text{local}}(p)$ are its moments, not its width. In this case the width of the distribution is irrelevant to its moments because it is not positive semidefinite. In fact, all of the moments of the local momentum transfer function (5.10) are zero, in a distributional sense [11]. Thus a particle confined to a single slit will suffer no transverse momentum disturbance, in agreement with the calculations of Scully *et al.* This is in contrast to *welcher Weg* experiments with classical momentum kicks, in which the single-slit momentum distribution variance must be increased by at least $(\hbar\pi/2d)^2$ if the double-slit interference pattern is to be destroyed, as shown in Sec. III C 2.

B. Two-valued projective scheme

In this section we consider an idealized projective measurement without a particular physical model for the apparatus. It can be considered as a limiting case of our model of the scheme of Scully *et al.* in which $\alpha\to 0$ and $\beta\to\infty$. That

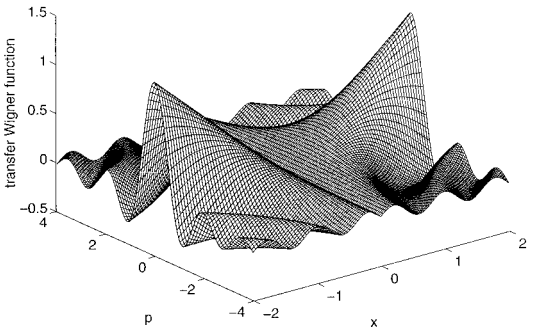

FIG. 11. Plot of $W_T(x,p)$ for a two-valued projective *welcher Weg* measurement.

is, the which-path measurement regions cover the entire x line. In this case there are just two possible measurement results $\xi=\pm$, described by the measurement functions

$$O_{\pm}(x)=H(\pm x), \tag{5.11}$$

where $H(x)$ is the Heaviside function as above. The Wigner function for $O_{+}(x)$ is

$$\begin{aligned} W_{O_+}(x,p)&=\frac{1}{\pi\hbar}\int dy\ H(x+y)H(x-y)e^{2iyp/\hbar}\\ &=\frac{1}{\pi\hbar}H(x)\int_{-x}^{x}dy\ e^{2iyp/\hbar}\\ &=\frac{1}{\pi\hbar}H(x)\frac{\sin(2px/\hbar)}{p/\hbar}. \end{aligned} \tag{5.12}$$

The total transfer Wigner function is thus

$$W_T(x,p)=\frac{1}{\pi p}\sin\frac{2|x|p}{\hbar}. \tag{5.13}$$

This Wigner function is plotted in Fig. 11 and is identical to that of Sec. V A in the limit $\alpha\to 0$ and $\beta\to\infty$.

The nonlocal momentum transfer function is

$$P_{\text{nonlocal}}(p)=\lim_{|x|\to 0}\frac{1}{\pi p}\sin\frac{2|x|p}{\hbar}=\lim_{|x|\to 0}\frac{2|x|}{\hbar\pi}=0. \tag{5.14}$$

This result appears to contradict our theorem stating that $P_{\text{nonlocal}}(p)\neq 0$ for some $p\geqslant\pi\hbar/2d$. It also fails to satisfy the normalization condition (3.10). These violations are artifacts of the infinitely sharp boundary between the two measurement regions. The way to interpret the result $P_{\text{nonlocal}}(p)=0$ is to consider $P_{\text{nonlocal}}(p)$ as an infinitely broad and hence infinitely low distribution. This can be understood from Eq. (5.8) for $P_{\text{nonlocal}}(p)$ in the scheme of Scully *et al.* In the limit as $\alpha\to 0$, this $P_{\text{nonlocal}}(p)$ becomes infinitely broad and infinitely low, but remains a normalized distribution. This distribution can transfer arbitrarily large momenta, as is necessary since the two-valued projective scheme will destroy the interference fringes no matter how small the slit separation d becomes.

In deriving our theorem regarding $P_{\text{nonlocal}}(p)$, we assumed in Sec. III B 2 that $W_T(x,p)$ was approximately constant as a function of x in a region of width a around $x=0$ (where $a\ll d$ is the slit width). For the transfer Wigner function for the two-valued projective measurement case (5.13), this is not the case since the characteristic p width of $W_T(x,p)$ diverges like $\hbar/|x|$ as $x\to 0$, which cannot be regarded as slowly varying no matter how small a is. Hence the destruction of interference is not by $P_{\text{nonlocal}}(p)=W_T(0,p)$ alone, but by $W_T(x,p)$ for $-a/2<x<a/2$. Providing $a\ll d$, the theorem (3.34) can be generalized to say that complete destruction of interference requires that $W_T(x,p)$ must not be identically zero for $-a/2<x<a/2$ and $p>\pi\hbar/2d$. It is clear from Eq. (5.13) and Fig. 11 that this is the case and that as $x\to 0$ the transfer function $W_T(x,p)$ becomes wider and flatter. From this context it can again be seen that $P_{\text{nonlocal}}(p)$ should be interpreted as an infinitely wide, infinitely flat distribution function.

In this two-valued projective measurement, the local momentum transfer distribution is

$$P_{\text{local}}(p)=\frac{1}{\pi p}\sin\frac{pd}{\hbar}. \tag{5.15}$$

As in the scheme of Scully *et al.*, this has a characteristic width of order $\hbar/d$, but its moments are all zero. In this case, it can be verified directly that a particle initially confined to the positive x axis is unaffected by the measurement. The initial wave function $\psi_i(x)$ of such a particle is 0 for all $x\leqslant 0$. Hence the initial Wigner function is

$$W_i(x,p)=\frac{1}{\pi\hbar}\int_{-x}^{x}dy\ \psi_i^*(x+y)\psi_i(x-y)e^{2ipy/\hbar}. \tag{5.16}$$

From Eq. (5.13), the final Wigner function is

$$\begin{aligned} W_f(x,p)&=\frac{1}{\pi\hbar}\int_{-x}^{x}dy\ \psi_i^*(x+y)\psi_i(x-y)e^{2ipy/\hbar}\\ &\quad\times\int dp'\,\frac{1}{\pi p'}\sin\frac{2|x|p'}{\hbar}e^{-2ip'y/\hbar}. \end{aligned} \tag{5.17}$$

The second integral evaluates to 1 if and only if $|y|<|x|$. As is apparent from the first integral, this is true for the initial state under consideration. Therefore,

$$W_f(x,p)=W_i(x,p), \tag{5.18}$$

so that the particle state is unchanged. Thus there is no momentum disturbance to a particle passing through one slit, as expected given that a projective measurement would have no effect if one already knew that the particle was on one side of the $x=0$ plane. A similar calculation could also be carried out for the scheme of Sec. V A.

C. The Storey-Collett-Walls scheme

We now consider a recent atom optics *welcher Weg* proposal, due to Storey, Collett, and Walls [25], whose analysis we shall draw upon here. An atom is prepared in the ground state, passes through two slits at $x=\pm d/2$, and then passes

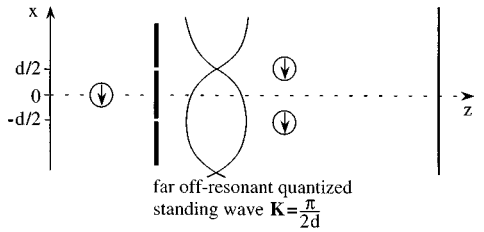

FIG. 12. Diagram of the Storey-Collett-Walls *welcher Weg* scheme. The atom remains in the ground state and produces a π phase shift on the field if it passes through the antinode and no phase shift if it passes through the node.

through a standing-wave light field of wave number $K=\pi/2d$ positioned so that the upper slit is in front of a node and the lower an antinode, as shown in Fig. 12. When the standing-wave frequency is detuned, by a large positive Δ, from the atomic transition frequency, the atom remains in the ground state throughout, but imparts a position-dependent phase shift to the field. As explained in [25], in a frame rotating at the field frequency, the effective interaction Hamiltonian in the regime of large detuning is

$$H=\hbar\frac{|g|^2}{\Delta}\sigma_3 a^\dagger a\cos^2K(x-x_0)+\hbar\Delta\sigma_3, \qquad (5.19)$$

where g is the one-photon Rabi frequency and $Kx_0=-Kd/2=-\pi/4$. After an interaction time t, the first term in this Hamiltonian will have changed the phase of the standing wave by an amount $(|g|^2t/\Delta)\cos^2K(x-x_0)$.

If the atom passes through a node, there is no phase shift, whereas if the atom passes through an antinode the phase of the field alters by an amount $|g|^2t/\Delta$. By choosing the interaction time so that the difference between the optical phase change induced by the two atomic paths is $\pi=|g|^2t/\Delta$, a phase-sensitive measurement of the field can act as a *welcher Weg* measurement for the atom. In order for this to work, the initial state must have a well-defined phase, and in Ref. [25] it is chosen to be a coherent state $|\alpha\rangle$. In this case the fringe visibility is given by the inner product of the final states entangled with the atomic position,

$$V=|\langle\alpha|-\alpha\rangle|=\exp[-2|\alpha|^2], \qquad (5.20)$$

which, as for the Einstein recoiling slit of Sec. IV A, can never be strictly zero.

For α real, a *welcher Weg* measurement can be performed by measuring the real quadrature of the field, while measuring the imaginary quadrature effects a quantum eraser [25]. Counting the number of photons in the field also constitutes a quantum eraser measurement since all phase information is destroyed in the process. Unlike quadrature measurements, this measurement has a discrete basis, so we choose it in order to calculate the transfer Wigner functions. We find

$$\begin{aligned}W_{O_n}(x,p)&=\frac{1}{\pi\hbar}\frac{|\alpha|^{2n}e^{-|\alpha|^2}}{n!}\int dy\ \exp\left[\frac{2ipy}{\hbar}\right]\\&\quad\times\exp[-in\pi\ \cos^2K(x+y-x_0)]\\&\quad\times\exp[in\pi\ \cos^2K(x-y-x_0)]\\&=\frac{|\alpha|^{2n}e^{-|\alpha|^2}}{\pi\hbar n!}\int dy\ \exp\left[\frac{2ipy}{\hbar}\right]\\&\quad\times\exp[in\pi\ \sin2K(x-x_0)\sin2Ky].\end{aligned} \qquad (5.21)$$

This integral evaluates to zero unless $p/\hbar K$ is an integer, in which case the integrand is periodic in $-\pi/2K<y<\pi/2K$. Using

$$\begin{aligned}&\int_{-\pi/2K}^{\pi/2K}dy\ \cos[n\pi\ \sin2K(x-x_0)\sin2Ky-m2Ky]\\&\quad=\pi K^{-1}J_m(n\pi\ \sin2K(x-x_0)),\end{aligned} \qquad (5.22)$$

where J_m is a Bessel function of integer order, we have

$$W_{O_n}(x,p)=\frac{|\alpha|^{2n}e^{-|\alpha|^2}}{\hbar Kn!}\sum_m\ \delta\left(\frac{2pd}{\hbar\pi}+m\right)J_m\left(n\pi\ \cos\frac{\pi x}{d}\right). \qquad (5.23)$$

We have substituted $Kx_0=-\pi/4$ and $Kd=\pi/2$ and are using the convention that the sum is over all integers unless otherwise indicated.

The total momentum transfer Wigner function is the sum over all photon numbers n:

$$W_T(x,p)=e^{-|\alpha|^2}\sum_{n\geq0,m}\frac{|\alpha|^{2n}}{n!}\delta\left(p+\frac{m\pi\hbar}{2d}\right)J_m\left(n\pi\ \cos\frac{\pi x}{d}\right). \qquad (5.24)$$

At the slits, where $x=\pm d/2$, the argument of the Bessel functions is identically zero for all n, so

$$P_{\rm local}(p)=\sum_m\ \delta(p+m\hbar K)J_m(0)=\delta(p), \qquad (5.25)$$

and there is absolutely no local momentum disturbance. This example is a clear demonstration that nonlocal momentum transfer is sufficient to destroy interference patterns. Figure 13 shows $W_T(x,p)$ for $\alpha=3/2$, chosen to give an unconditioned fringe visibility of about 1% [Eq. (5.20)]. As this plot shows, $W_T(x,p)$ is not positive semidefinite, and this is true for all α. The asymmetry in p for this transfer Wigner function favors negative momentum transfers in the region between the slits. This can be understood in that an atom passing through the antinode at the lower slit experiences a positive potential that retards (i.e., makes more negative) its temporal phase relative to one passing through the node at the upper slit. This phase differential would tend to ''kick'' an atom passing between these two points towards negative x, but it is certainly not a classical kick. As is apparent from

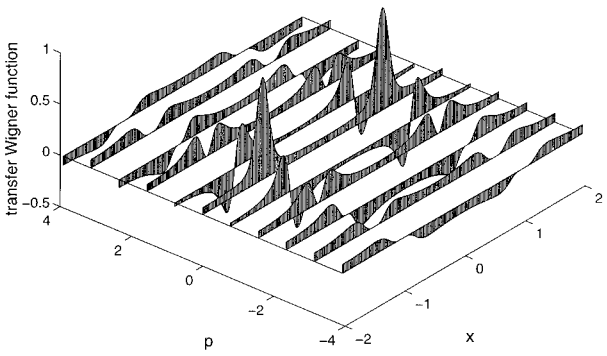

FIG. 13. Plot of $W_T(x,p)$ for the Storey-Collett-Walls *welcher Weg* scheme. As usual, the slits are located at $x=\pm 1$. The heights have been scaled such that a δ function has height 1. We have not plotted those points where $W_T(x,p)=0$ in order to display the function more clearly.

Fig. 13, the nonlocal momentum transfer is certainly wide enough to satisfy the theorem (3.34).

D. Scheme with non-negative but nonclassical $W_T(x,p)$

We now consider an alternative method of *welcher Weg* detection of an atom initially in the ground state. In this case, the slits are immediately in front of two adjacent antinodes of a resonant standing-wave classical light field of wave number $K=\pi/d$, as shown in Fig. 14. Ignoring spontaneous emission [24], the Hamiltonian describing the atom-field interaction is $H=\hbar\Omega\sigma_1\sin Kx$, so evolution of the state of the atom while in the field is described by the unitary time evolution operator

$$U(t)=\exp[-i\Omega t\sigma_1\sin Kx]. \tag{5.26}$$

To make a perfect *welcher Weg* measurement the interaction time is taken to be $\Omega t=\pi/4$. This produces orthogonal internal states of the atom at the upper and lower slits. The final state of the atom is

$$|\Psi\rangle=\int dx\ \exp\left[-i\frac{\pi}{4}\sigma_1\sin Kx\right]\psi(x)|x\rangle|g\rangle. \tag{5.27}$$

To determine which way the atom went, the internal state is measured in the $\sigma_2=i|g\rangle\langle e|-i|e\rangle\langle g|$ basis. The result $\sigma_2=-1$ corresponds to the atom being in the state $1/\sqrt{2}(|g\rangle-i|e\rangle)$ and having taken the upper path and

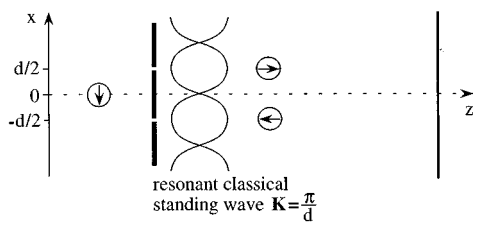

FIG. 14. Diagram of the *welcher Weg* scheme of Sec. V D. The atom begins in the ground state and its internal states act as the *welcher Weg* detectors. A left arrow denotes a state with $\sigma_2=+1$ and a right arrow one with $\sigma_2=-1$.

$\sigma_2=+1$ corresponds to it being in the state $1/\sqrt{2}(|g\rangle+i|e\rangle)$ and having taken the lower path.

As in earlier sections, it is easier to calculate the Wigner functions in the basis that erases the *welcher Weg* information, in this case the σ_1 basis. The two possible outcomes from measuring σ_1 are described by

$$O_{\pm}(x)=\pm\frac{1}{\sqrt{2}}\exp\left[\mp i\frac{\pi}{4}\sin Kx\right]. \tag{5.28}$$

The Wigner function for $O_+(x)$ is

$$W_{O_+}(x,p)=\frac{1}{2\pi\hbar}\int dy\ \exp\left[i\frac{\pi}{2}\cos Kx\ \sin Ky+\frac{2ipy}{\hbar}\right]. \tag{5.29}$$

Using the same technique as in Sec. V C we find

$$W_{O_+}(x,p)=\frac{1}{2}\sum_m\ \delta\left(p+\frac{1}{2}m\hbar K\right)\ J_m\left(\frac{\pi}{2}\cos Kx\right). \tag{5.30}$$

The Wigner function for the other measurement outcome is

$$W_{O_-}(x,p)=\sum_m\ \delta\left(p+\frac{1}{2}m\hbar K\right)J_m\left(-\frac{\pi}{2}\cos Kx\right). \tag{5.31}$$

For even m, $J_m(y)=J_m(-y)$, whereas for odd m, $J_m(y)=-J_m(-y)$, so in adding $W_{O_+}(x,p)$ and $W_{O_-}(x,p)$ to obtain $W_T(x,p)$, the odd terms vanish. The total momentum transfer Wigner function is

$$W_T(x,p)=\sum_m\ \delta(p+m\hbar\pi/d)\ J_{2m}\left(\frac{\pi}{2}\cos\frac{\pi x}{d}\right), \tag{5.32}$$

where the substitution $Kd=\pi$ has been made. This is plotted in Fig. 14. Since the modulus of the argument of the Bessel functions is bounded by $\pi/2$, each term in the sum of Eq. (5.32) is non-negative. Therefore, this $W_T(x,p)$ is non-negative everywhere, a feature different from the preceding quantum schemes. Nevertheless, this $W_T(x,p)$ cannot be interpreted in a classical way as a probability distribution for position-dependent local momentum kicks. This is because the momentum transfer at the slits is zero [with $P_{\rm local}(p)=\delta(p)$ as in Sec. V C], so that the destruction of interference can only be understood in terms of the nonlocal momentum transfer in the region between the slits. Hence we conclude that the positivity of the transfer Wigner function is not sufficient for it to have an interpretation in terms of classical momentum kicks; this example reaffirms the definition for classical momentum kicks established in Sec. II.

The nonlocal momentum transfer function at $x=0$ is

$$P_{\rm nonlocal}(p)=\sum_m\ \delta(p+m\pi\hbar/d)J_{2m}(\pi/2). \tag{5.33}$$

As is apparent from Fig. 15, this is well approximated by

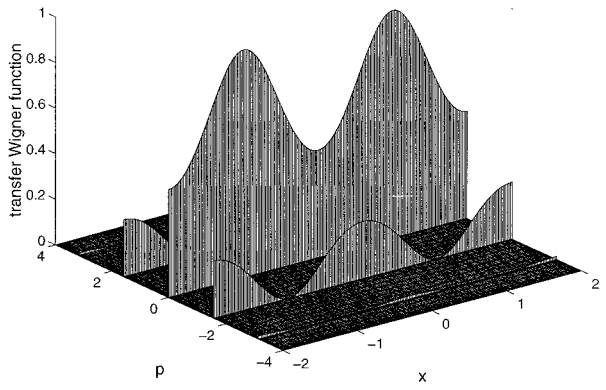

FIG. 15. Plot of $W_T(x,p)$ for the *welcher Weg* scheme of Sec. V D. As in Fig. 13, a height of unity represents a δ function, and the slits are located at $x=\pm 1$.

$$P_{\text{nonlocal}}(p)\approx\frac{1}{4}\delta(p+\pi\hbar/d)+\frac{1}{2}\delta(p)+\frac{1}{4}\delta(p-\pi\hbar/d). \tag{5.34}$$

This destroys the interference pattern by adding two 1/4 height patterns in antiphase with the original pattern to a 1/2 height replica of the original pattern. This can be compared with the explanation for the destruction of interference in Sec. IV C, but it must be remembered that in contrast to that classical case, the quantum scheme presented here destroys the interference pattern without broadening the diffraction envelope.

We have conclusively shown that a nonlocal momentum disturbance is all that is required to destroy the interference pattern. In Appendix C we use this example to show that the converse is true as well: the interference pattern may be completely preserved even if there are local momentum transfers.

VI. EXPERIMENTAL SIGNATURES OF NONLOCAL MOMENTUM TRANSFER

While the transfer Wigner function $W_T(x,p)$ is unparalleled in its ability to represent any *welcher Weg* measurement experiment in terms of momentum disturbance, it is not directly discernible from the results of experiments. In this section we look more closely at the experimental signatures of the various *welcher Weg* schemes we have investigated.

A. Momentum transfer to a momentum eigenstate

The reason the transfer Wigner function $W_T(x,p)$ is not experimentally observable is that it is only a pseudoprobability distribution function. This is highlighted by the fact that it is not always positive semidefinite (see Secs. V A–V C), so cannot strictly be interpreted as the probability for a particle at position x to receive a momentum kick of magnitude p. It would be a cause for considerable alarm if one could put a particle at position x and observe that it has a negative probability for receiving certain momentum kicks. Physically, the reason that one cannot do this is that if one were to localize a particle to a point then its momentum uncertainty would become infinite. Hence there would be no possible way in which any momentum disturbance could be detected. Any state with a well-defined initial momentum will necessarily have a sufficiently wide position distribution that the negative parts of $W_T(x,p)$ are smeared out so that the final momentum distribution is non-negative.

Since exact momentum transfers can only be observed if the initial state has no momentum spread, one could argue that the best way to define the momentum transfer distribution function of any *welcher Weg* scheme is to calculate the final momentum distribution of a state initially in the eigenstate $p=0$. This means the initial wave function is flat in position and the initial Wigner function is $W_i(x,p)\propto\delta(p)$. Thus the final Wigner function is

$$W_f(x,p)\propto W_T(x,p) \tag{6.1}$$

and the final momentum distribution is the marginal p distribution for $W_T(x,p)$,

$$P_T(p)\propto\int dx\ W_T(x,p). \tag{6.2}$$

It is simple to show further that

$$\int dx\ W_T(x,p)=\sum_{\xi}|\widetilde{O}_{\xi}(p)|^2, \tag{6.3}$$

so that $P_T(p)$ can be defined independently of the momentum transfer Wigner function. The theorem of Storey *et al.* that at least one $\widetilde{O}_{\xi}(p)$ must be nonzero for some $p>\hbar/d$ [6], together with Eq. (6.3), implies that $P_T(p)$ must obey the same constraint, provided the integrals exist. By using the theorem of Boas rather than Bernstein, as we have done in Sec. III C 1, this lower bound can be increased from $\hbar/d$ to $\pi\hbar/2d$.

For the case of classical momentum kicks $P_T(p)=P_{\text{local}}(p)=P_{\text{nonlocal}}(p)$, so we already know $P_T(p)$ for these cases. The quantum cases are more interesting. In the case of the two-valued projective measurement of Sec. V B,

$$P_T(p)=\mathcal{N}\int dx\,\frac{1}{\pi p}\sin\frac{2|x|p}{\hbar}, \tag{6.4}$$

where the constant of proportionality $\mathcal{N}$ is required for normalization. Since the integral is divergent, a distributional approach is required. We introduce an apodization function, such as $e^{-2\gamma|x|}$, in the integrand, carry out the normalization, and finally let $\gamma\to 0$ after calculating physical quantities of interest. Thus we write

$$P_T(p|\gamma)=\mathcal{N}\int dx\,\frac{1}{\pi p}\sin\frac{2|x|p}{\hbar}e^{-2\gamma|x|}, \tag{6.5}$$

which after normalization yields

$$P_T(p|\gamma)=\frac{1}{\pi}\,\frac{\hbar\gamma}{p^2+\hbar^2\gamma^2}. \tag{6.6}$$

For every nonzero value of γ, this function is not supported only in the interval $[-\pi\hbar/2d,\pi\hbar/2d]$, as required by the theorem. Furthermore, all even moments of $P_T(p|\gamma)$ are infinite, indicating that an infinite amount of momentum uncer-

tainty is introduced. These results do not depend on the exact form of the apodization function used.

In the limit $\gamma\to 0$, although $P_T(p|\gamma)$ formally tends to the distributional limit $\delta(p)$, this must be interpreted carefully, since the support and variance of a δ ''function'' depend on the sequence of functions that are used to approximate to it, and are not well-defined concepts in general. These problems are not present in the δ functions that appear in $W_T(x,p)$ for the schemes analyzed in Secs. IV C, V C and V D because the measurement wave functions $O_\xi(x)$ in those cases are smooth functions of x, unlike the $O_\pm(x)=H(\pm x)$ for the two-valued projective case. The physical significance of the infinite variance of the result obtained above by apodization [Eq. (6.6)] is that for any initial state that is close to a momentum eigenstate (and, in particular, that could have an arbitrarily small momentum variance), the output state will have an infinite momentum variance. This can be verified by direct calculation from the measurement wave functions $O_\pm(x)$ for the two-valued projective measurement (5.11).

The scheme of Scully *et al.* in Sec. V A also leads to a divergent integral for $P_T(p)$ similar to Eq. (6.4) because of the assumed infinite extent of the apparatus. Regularizing that integral in a similar way leads to the same results that for all nonzero values of γ, $P_T(p|\gamma)$ is not supported only in the interval $[-\pi\hbar/2d,\pi\hbar/2d]$ and all even moments of $P_T(p|\gamma)$ are infinite. Again, this indicates that the root-mean-square momentum transferred by the apparatus of Scully *et al.* to a momentum eigenstate is infinite.

The other two quantum schemes we considered are not pathological because their apparatuses are smooth and periodic in x. For the scheme of Sec. V C, based on an optical phase measurement, the momentum transfer for $p=m\hbar K$ with m odd will average to zero, as can be verified from Eq. (5.24). This makes the distribution $P_T(p)$ nonzero only for momentum transfers equal to even multiples of the photon momentum, as expected for diffraction from a far-detuned standing wave [26]. For the scheme of Sec. V D, $W_T(x,p)$ is nowhere negative so that there will be no cancellation of momentum transfers. In this case the marginal distribution is

$$P_T(p)\propto\sum_m \delta(p-m\hbar\pi/d)\int dx\; J_{2m}\left(\frac{\pi}{2}\cos\frac{\pi x}{d}\right). \tag{6.7}$$

This clearly does give momentum transfer in excess of $p_m=\hbar\pi/2d$. The integrals can be evaluated numerically and the standard deviation of the total momentum disturbance is

$$\sigma_T(p)\approx 1.74\hbar/d. \tag{6.8}$$

The fact that $P_T(p)$ is nonzero for some $p\geqslant\pi\hbar/2d$ for all cases suggests that the momentum transferred to a momentum eigenstate is insensitive to the distinction between quantum and classical momentum transfers. However, this is not necessarily the case. For the *welcher Weg* schemes with classical momentum transfer, $P_T(p)=P_{\rm nonlocal}(p)$. This means that not only must there be some momentum transfer to a momentum eigenstate greater than $p_m=\pi\hbar/2d$, but the probability distribution $P_T(p)$ for that momentum transfer must obey the same integral condition (3.20) as $P_{\rm nonlocal}(p)$. That is, if there is to be complete destruction of interference in the two-slit case, then

$$\int e^{ipd/\hbar}P_T(p)dp=0. \tag{6.9}$$

In the quantum cases, this need not hold. In fact, in the two-valued projective measurement and the Scully-Englert-Walther scheme, the integral evaluates to $e^{-\gamma d}$, which goes to unity as the apodization parameter γ goes to 0. The other quantum cases are less extreme, but both give a nonzero result for the integral in Eq. (6.9). This shows that $P_T(p)$ can distinguish between quantum and classical momentum transfers, at least for the examples considered in this paper.

B. Form of the momentum distribution

Although the momentum transferred to a momentum eigenstate, with the distribution $P_T(p)$, may be able to distinguish quantum and classical momentum transfers, this is a rather indirect signature. As we have discussed above, however, there is a direct signature in the interference pattern itself, in that classical momentum kicks will necessarily broaden the diffraction envelope whereas quantum momentum transfers need not. This is most apparent if one allows the ratio of the slit width a to the slit separation d to be finite rather than tending to zero as we have assumed in all previous analyses. The simplest cases to look at are the minimally disturbing atom optics scheme of Sec. IV C and the two-valued projective measurement of Sec. V B. The other quantum and classical cases are very similar.

The initial state of a particle emerging from double slits of width a is

$$\psi_i(x)=\frac{1}{\sqrt{2a}}[\chi_{(-d/2-a/2,-d/2+a/2)}(x)+\chi_{(d/2-a/2,d/2+a/2)}(x)], \tag{6.10}$$

where $\chi(x)$ denotes a characteristic function as in Sec. V A. In momentum space this superposition becomes

$$\tilde{\psi}_i(p)=\sqrt{\frac{a}{\pi\hbar}}\,\frac{\sin[ap/2\hbar]}{ap/2\hbar}\cos\frac{pd}{2\hbar}, \tag{6.11}$$

so the initial momentum probability distribution is

$$P_i(\wp)\propto\mathrm{sinc}^2(\zeta\wp)\cos^2(\pi\wp/4). \tag{6.12}$$

Here we have scaled p as $\wp=p/p_m$ and a as $\zeta=a/4d$ and introduced $\mathrm{sinc}x=(\pi x)^{-1}\sin\pi x$. We have plotted this distribution for $a=0.4d$ in Fig. 16. It describes a double-slit interference pattern within a single-slit diffraction envelope.

For the classical case of Sec. IV C the particle receives with equal probability momentum kicks of $\pm\hbar\pi/2d$. This transforms the wave function (6.11) into

$$\tilde{\psi}_\pm(\wp)\propto\mathrm{sinc}[\zeta(\wp\mp 1)]\cos[\pi(\wp\mp 1)/4]. \tag{6.13}$$

The final momentum distribution is

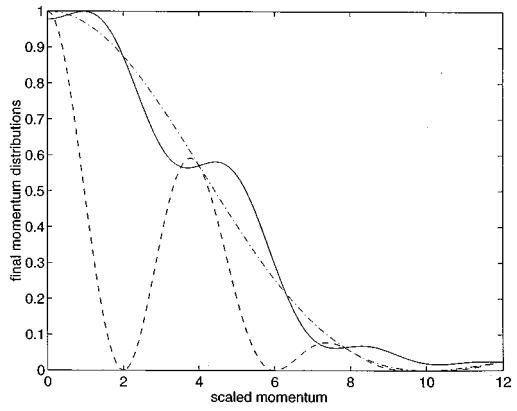

FIG. 16. Plot of final momentum distributions for the case of no measurement (identical to the initial momentum distribution) (dashed line), a nonlocal quantum scheme (the projective measurement of Sec. V B) (dash-dotted line), and a local classical scheme (the minimally disturbing measurement of Sec. IV C) (solid line). The momentum is scaled as $\wp = 2pd/\hbar\pi$ so that the minimum disturbance is to change $\wp$ by ± 1. The slits have width $a = 0.4d$.

$$P_f(\wp) \propto \frac{1}{2}\{\mathrm{sinc}^2[\zeta(\wp-1)] - \mathrm{sinc}^2[\zeta(\wp+1)]\}\sin\frac{\pi\wp}{2} + \frac{1}{2}\{\mathrm{sinc}^2[\zeta(\wp-1)] + \mathrm{sinc}^2[\zeta(\wp+1)]\}. \quad (6.14)$$

In the limit of zero slit width, $\zeta \to 0$ and the second term here becomes equal to unity while the first vanishes. For nonzero ζ the first term does not vanish and so there are residual interference fringes. This is because the momentum kicks destroy interference between points in the wave function a distance exactly d apart, but the initial particle wave function has coherences at all distances between $d-a$ and $d+a$. The distribution (6.14) is also plotted in Fig. 16. Note that the first zero of the single-slit diffraction pattern has been filled in by the momentum kicks. This smearing of the diffraction envelope is the signature of the local momentum kicks.

The quantum cases give a quite different result. The projective measurement of Sec. V B determines whether or not the particle goes above or below the center point $x = 0$. The wave function after the measurement is thus

$$\psi_{\pm}(x) = \frac{1}{\sqrt{a}}\chi_{(\pm d/2 - a/2, \pm d/2 + a/2)}(x), \quad (6.15)$$

where the result $\pm$ denotes the sign of x in the appropriate half line. Both of these wave functions have the momentum distribution characteristic of single-slit diffraction, so the far-field pattern is

$$P_f(\wp) \propto \mathrm{sinc}^2(\zeta\wp), \quad (6.16)$$

which is shown in Fig. 16. This shows that a quantum *welcher Weg* scheme can destroy the interference pattern without altering the diffraction pattern at all. This is an unambiguous experimental signature of the nonlocal nature of the momentum transfer in such *welcher Weg* schemes.

C. The Aharonov-Bohm effect

There is an interesting analogy between the analysis of this section and the nonlocality of the Aharonov-Bohm effect [27,28]. Aharonov and Bohm presented two versions of their effect: a magnetic one and an electric one [27]. In the former (which is better known) a magnetic solenoid is placed between the two slits, with its axis perpendicular to the line of the slits and the longitudinal motion of the particle. Even though the magnetic field is zero in the region of the slits, it nevertheless influences the interference fringes if the particle is charged. Rather than destroying the fringes, the magnetic field inside the solenoid merely induces a phase shift of $\phi = (e/\hbar c)AB$, where A is the cross-sectional area of the solenoid and B the magnetic field strength.

As pointed out by Boyer [29] and Fearn [30], the diagram showing this fringe shift in the Feynman lectures [31] is wrong. The error is that the entire interference pattern is shown as being shifted, whereas what actually happens is that the interference fringes move *within* the diffraction envelope, which stays constant. We bring this up in order to make the connection with our current work. A classical momentum transfer due to a deterministic force from a local electromagnetic field would result in a shift of the entire pattern, in the same way as a classical or local *welcher Weg* measurement smears the entire pattern. By contrast, the Aharonov-Bohm effect, like a quantum or nonlocal *welcher Weg* measurement, affects only the interference fringes themselves.

For comparison with the *welcher Weg* schemes, the Aharonov-Bohm effect can also be described using the Wigner function formalism, at least phenomenologically. Treating the longitudinal motion of the electron classically as usual, the effect of the solenoid at $x = 0$ can be modeled as giving a relative phase shift of ϕ between all particles with $x < 0$ and all particles with $x > 0$. This is effected by multiplying the particle wave function by

$$O_\phi(x) = H(x)e^{i\phi} + H(-x), \quad (6.17)$$

the momentum transfer Wigner function of which can be evaluated using the theory of distributions to be

$$W_T^\phi(x,p) = \delta(p)\cos\phi + \frac{\sin(2p|x|/\hbar)}{\pi p}(1-\cos\phi) + \frac{\cos(2px/\hbar)}{\pi p}\sin\phi, \quad (6.18)$$

where have used $W_T^\phi(x,p)$ for $W_{O_\phi}(x,p)$. It can be verified that this is normalized as usual for all $x \neq 0$. The nonlocal momentum transfer function is found by setting $x = 0$ to get

$$P^\phi_{\mathrm{nonlocal}}(p) = \delta(p)\cos\phi + (\pi p)^{-1}\sin\phi. \quad (6.19)$$

This is not normalizable (an artifact of the infinitely sharp boundary, as in Sec. V B), but does give the correct complex visibility

$$\mathcal{V} = \int dp\ e^{ipd/\hbar}[\delta(p)\cos\phi + (\pi p)^{-1}\sin\phi] = e^{i\phi}. \quad (6.20)$$

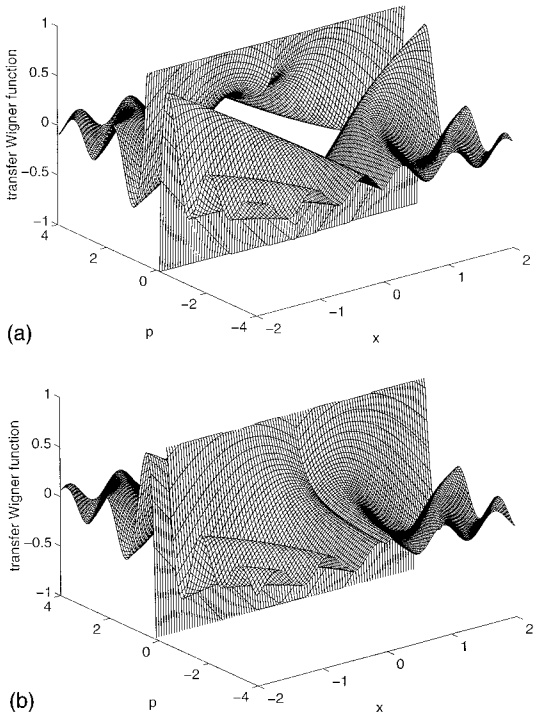

FIG. 17. Plot of $W_T(x,p)$ for the Aharonov-Bohm effect, in which the phase difference ϕ between the upper and lower half planes is (a) $\pi/2$ and (b) $-\pi/2$. The function diverges as $p\to 0$ from above and below.

For the cases $\phi=\pm\pi/2$, Eq. (6.18) gives the momentum transfer Wigner functions

$$W_T^{\pm\pi/2}(x,p)=\frac{\sqrt{2}}{\pi p}\sin\left(\frac{2p|x|}{\hbar}\pm\frac{\pi}{4}\right). \tag{6.21}$$

These are plotted in Fig. 17. There are obvious similarities to the transfer function for the two-valued projective measurement of Sec. V B. Indeed, for all ϕ,

$$\frac{1}{2}[W_T^{\phi}(x,p)+W_T^{\phi+\pi}(x,p)]=\frac{1}{\pi p}\sin\frac{2|x|p}{\hbar}, \tag{6.22}$$

which is equal to $W_T(x,p)$ for the projective case (5.13). This is because adding one fringe pattern to its antiphase pattern effaces the fringes. This is directly relevant to the Scully-Englert-Walther scheme of Sec. V A. In order to find out which path the atom took, one would measure which microwave cavity contained the photon. In terms of the photon number states of the cavities this would have the measurement basis $\{|0_1\rangle|1_2\rangle,|1_1\rangle|0_2\rangle\}$. On the other hand, as pointed out by Scully *et al.* [3], measurement in a complementary basis such as $\{|0_1\rangle|1_2\rangle\pm i|1_2\rangle|0_2\rangle\}$ constitutes a quantum eraser. In this case one sees perfect fringes, shifted by $\pi/2$ or $-\pi/2$. In the limit where the scheme of Scully *et al.* approaches the two-valued projective measurement, the transfer Wigner functions for these two results are precisely those plotted here for the Aharonov-Bohm effect. In fact, the Scully-Englert-Walther scheme has been analyzed by Bhandari in terms of a random geometric phase [19].

The phenomenological treatment of the Aharonov-Bohm effect through Eq. (6.17) describes more closely the electric, rather than the magnetic, Aharonov-Bohm effect [27]. In this version the two paths the electron may take pass through hollow conducting cylinders as shown in Fig. 18. While the electron wave packet is wholly enclosed within the cylinders, a voltage source is switched on, creating a potential difference V between the two cylinders. This remains on for time t, giving a phase difference of $\phi=eVt/\hbar$ between the two paths. The voltage must be turned off before the wave packets exit the cylinders. This ensures that the electron never passes through a spatially varying potential and hence never experiences an electric field. Thus, as in the magnetic version, the phase difference is a nonlocal, topological effect not due to any local electromagnetic forces.

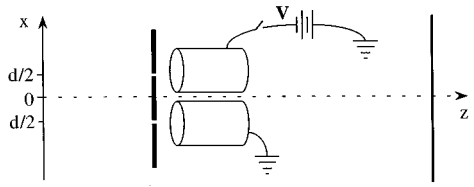

FIG. 18. Diagram of the electric Aharonov-Bohm effect.

To justify a strict analogy with the Aharonov-Bohm effect, the nonlocal *welcher Weg* measurements analyzed here would have to be implemented in such a way that the particle never experiences any potential gradients. Otherwise, one could see the effect of a measurement on a particle traveling through a single slit: even though the particle leaves the region of the potential with the same velocity with which it entered, the position of its wave packet would be retarded or advanced in addition to its phase being retarded or advanced. This can be avoided in the same way as in the electric Aharonov-Bohm effect. The coupling to the apparatus would be turned on only when the particle is in the region where that coupling is constant as a function of longitudinal position and turned off before it leaves that region. For our proposal of Sec. V D it is easy to see how this can be done; the classical standing wave that couples the position of the atom to the apparatus (its internal states) can be created and removed simply by controlling the direction of a laser beam. This technique has already been used experimentally to control interaction times of slow-moving atoms in laser fields [32]. For the other nonclassical schemes of Sec. V it is less obvious how this switching might be achieved, but it is presumably possible.

VII. CONCLUSION

The destruction of interference fringes in a *welcher Weg* measurement must be accompanied by some momentum transfer at least equalling $p_m=\pi\hbar/2d$. In the older, well-known *welcher Weg* schemes this momentum transfer can be interpreted as random classical momentum kicks, with the particle's momentum probability distribution being convolved with a momentum transfer probability distribution. In these cases p_m is also the minimum for the standard deviation of the momentum transfer distribution. In some more recent schemes this picture fails and the momentum disturbance requires a quantum-mechanical description, in terms of amplitudes rather than probabilities.

The Wigner function formalism allows both quantum and classical momentum transfer to be treated on the same footing. The momentum transfer Wigner function $W_T(x,p)$, although it may be negative in places, formally plays the role of the probability distribution for a particle at position x to receive a momentum transfer p. In this formalism the interference fringes are destroyed by convolution with the momentum transfer function midway between the slits rather than at the slits. It is this nonlocal transfer function that we have shown must be nonzero for some $p \geq p_m$.

For *welcher Weg* schemes involving classical momentum transfer, $W_T(x,p)$ is non-negative and independent of x, so that the momentum disturbance that destroys the interference also acts locally, at the slits. Thus one can treat the destruction of the fringes as if it were a local effect. However, for quantum cases the momentum disturbance at the slits can be precisely zero. We conclude that the momentum transfer in these cases is inherently nonlocal. It is interesting to note that the positivity of the transfer Wigner function is not an indication of its classicality; we propose a scheme in which $W_T(x,p)$ is nowhere negative but equals $\delta(p)$ at the slit positions.

One experimental signature of the distinction between local and nonlocal momentum transfer can be seen for the slit width a finite relative to the slit separation d. When classical momentum kicks destroy the interference fringes, the entire pattern is smeared, including the diffraction pattern due to the finite a. For quantum *welcher Weg* schemes the interference fringes can be destroyed without altering the diffraction envelope at all. There is a close analogy to the Aharonov-Bohm effect, in which the interference fringes move within the diffraction envelope, in the absence of any electromagnetic forces. That the Aharonov-Bohm effect is almost universally recognized as a nonlocal quantum phenomenon indicates that the loss of visibility without local momentum kicks in some *welcher Weg* schemes should also be regarded in this way.

ACKNOWLEDGMENTS

This project was supported by the Marsden Fund of the Royal Society of New Zealand, the University of Auckland Research Committee, and the Australian Research Council.

APPENDIX A

Let the Fourier transform of $A(x)$ be denoted

$$\widetilde{A}(k) = \frac{1}{2\pi}\int dx\ e^{-ikx}A(x).$$

We define $\mathcal{B}(K)$ to be the class of all functions $A(x)$ such that $\widetilde{A}(k)$ is no more singular than a δ function and is supported only on the closed interval $[-K,K]$.

Lemma. Let $f(x) \in \mathcal{B}(K)$ be a real function of x satisfying $|f(x)| \leq 1 \quad \forall x$. Then

$$[f'(x)]^2 + K^2[f(x)]^2 \leq K^2 \quad \forall x.$$

Proof. See [12].

Theorem. No complex function $A(x)$ satisfying the conditions

$$A(0)=1, \quad A(d)=\mathcal{V}, \quad |A(x)| \leq 1 \quad \forall x \qquad \text{(A1)}$$

is contained in $\mathcal{B}(K)$ for any $K < \arccos(V)/d$, where $V=|\mathcal{V}|<1$.

Proof. Let $A(x) \in \mathcal{B}(K)$ satisfy the three conditions (A1). Now let $f(x)=\mathrm{Re}A(x)$. Then $f(x) \in \mathcal{B}(K)$ and from the lemma

$$\frac{f'(x)}{\sqrt{1-[f(x)]^2}} \leq K \quad \forall x.$$

Consider the smallest positive x_1 for which $f(x_1)=V$. Define a new function

$$F(x) = \arccos f(x).$$

Then $F(0)=0$ and $F(x_1)=\arccos V$. For $x \in (0,x_1)$,

$$F'(x) = \frac{f'(x)}{\sqrt{1-[f(x)]^2}} \leq K.$$

In this region $F(x) \leq Kx$ so that $x_1 \geq \arccos(V)/K$. Since $A(d)=\mathcal{V}$, $f(d) \leq V$ and so $d \geq x_1$. Thus $K \geq \arccos(V)/d$, completing the proof.

For the physical situations we consider, $\widetilde{A}(k)$ is no more singular than a δ function. Therefore, we can conclude that $\widetilde{A}(k)$ is not supported only on $[-K,K]$ for $K<\arccos(V)/d$. For the case $\mathcal{V}=V \geq 0$ the function $A(x)=\cos[\arccos(V)x/d]$ satisfies the three conditions (A1) and is of class $\mathcal{B}(K)$ for $K=\arccos(V)/d$. In particular, the lower bound $\pi/2d$ for $\mathcal{V}=0$ is in fact the minimum.

APPENDIX B

Theorem. Any non-negative function $P(k)$ satisfying the conditions

$$\int dk\ P(k)=1, \qquad \int dk\ P(k)e^{ikd}=\mathcal{V}$$

has a variance satisfying

$$\sigma^2 \equiv \int dk\ P(k)(k-\overline{k})^2 \geq [\arccos(V)/d]^2,$$

where $\overline{k}=\int dk\ P(k)k$ and $V=|\mathcal{V}| \leq 1$. Furthermore, the equality can be achieved for any $\mathcal{V}$.

Proof. If $\mathcal{V}=V$, then a symmetric distribution [satisfying $P(k)=P(-k)$] will minimize the variance. In this case $\overline{k}=0$ and

$$\sigma^2 = E_P[k^2], \qquad V=E_P[\cos(kd)], \qquad \text{(B1)}$$

where $E_P[\eta]$ denotes the expectation value of a random variable $\eta(k)$ with respect to the probability distribution $P(k)$. It is easy to verify that (i) $\eta^2 \geq [\arccos(\cos\eta)]^2$ for all real η and (ii) the function $f(\eta)=(\arccos\eta)^2$ is convex on the domain $-1 \leq \eta \leq 1$. It follows that for any random variable η, $f(E[\eta]) \leq E[f(\eta)]$. Using $\eta(k)=\cos(kd) \in (-1,1)$ we thus have

$$(\arccos\{E_P[\cos(kd)]\})^2 \leqslant E_P(\{\arccos[\cos(kd)]\}^2) \leqslant E_P(k^2d^2),$$

where we have used property (i). Substituting the definitions (B1) into this inequality yields the desired result.

If $\mathcal{V} \neq V$, define $Q(k)=P(k+\arg(\mathcal{V})/d)$ so that $\int dk\ Q(k)e^{ikd}=V$. Then for a minimum variance we require that $Q(k)=Q(-k)$ so that $k=-\arg(\mathcal{V})/d$ and $\sigma^2=\int dk\ Q(k)k^2$. The argument then follows as above with $P(k)$ replaced by $Q(k)$. This completes the proof.

The equality holds if the probability density of $\cos(kd)$ is a δ function, which is the case if the probability density of k consists of two δ functions symmetrically placed about k.

APPENDIX C

To show that an interference pattern may be completely preserved even if there is a local momentum disturbance, we consider the experiment described in Fig. 14, but with the slits placed at $x=0$ and $x=d$ (that is at the nodes rather than the antinodes). This configuration cannot be used to make a *welcher Weg* measurement, but the transfer Wigner function is the same as in the configuration of Sec. V D. From the plot of this function in Fig. 15 it can be seen that in this case there are local momentum transfers at the slits, but no disturbance midway between the slits (at $x=d/2$). Thus the interference pattern remains intact, even though the single-slit diffraction pattern will be smeared by the local momentum transfers.

This can be understood intuitively as follows. The atoms are initially in the ground state, which is a superposition of the eigenstates $|\pm\rangle$ of σ_1. These eigenstates experience the Hamiltonian $H=\pm\hbar\Omega\ \sin Kx$. At the lower slit ($x=0$), the $|+\rangle$ eigenstate is deflected downward and the $|-\rangle$ eigenstate is deflected upward. The upper slit is a mirror image, reflected in the plane $x=d/2$. Thus the $|+\rangle$ component of the atomic wave function will still form a symmetric interference pattern, as will the $|-\rangle$ component. The $|+\rangle$ component does not interfere with the $|-\rangle$ component, so the net result is that the interference fringes are still perfect and symmetric. This is despite the fact that the local momentum transfer distribution [which for this configuration is equal to the nonlocal distribution for the *welcher Weg* configuration, given in Eq. (5.33)] has a standard deviation of $\sigma_{\rm local}(p)\approx 2.47\hbar/d$.

[1] N. Bohr, in *Albert Einstein: Philosopher-Scientist*, edited by P.A. Schlipp (Library of Living Philosophers, Evaston, 1949), pp. 200–241 [reprinted in *Quantum Theory and Measurement*, edited by J.A. Wheeler and W.H. Zurek (Princeton University Press, Princeton, 1983), pp. 8–49].

[2] R.P. Feynman, R.B. Leighton, and M. Sands, *The Feynman Lectures on Physics* (Addison Wesley, Reading, MA, 1965), Vol. III.

[3] M.O. Scully, B.-G. Englert, and H. Walther, Nature (London) **351**, 111 (1991).

[4] B.-G. Englert, H. Fearn, M.O. Scully, and H. Walther, in *Quantum Interferometry*, edited by F. Martini, G. Denardo, and A. Zeilinger (World Scientific, Singapore, 1994), pp. 103–119; E.P. Storey, S.M. Tan, M.J. Collett, and D.F. Walls, *ibid.*, pp. 120–129.

[5] B.-G. Englert, M.O. Scully, and H. Walther, Nature (London) **375**, 367 (1995); E.P. Storey, S.M. Tan, M.J. Collett, and D.F. Walls, *ibid.* **375**, 368 (1995).

[6] E.P. Storey, S.M. Tan, M.J. Collett, and D.F. Walls, Nature (London) **367**, 626 (1994).

[7] H.M. Wiseman and F.E. Harrison, Nature (London) **377**, 584 (1995).

[8] V.B. Braginsky and F.Y. Khalili, *Quantum Measurement* (Cambridge University Press, Cambridge, 1992).

[9] E.B. Davies, *Quantum Theory of Open Systems* (Academic, London, 1976).

[10] E.P. Wigner, Phys. Rev. **40**, 749 (1932).

[11] A.H. Zemanian, *Distribution Theory and Transform Analysis* (McGraw-Hill, New York, 1965).

[12] R.P. Boas, Trans. Am. Math. Soc. **40**, 287 (1936).

[13] S. Bernstein, C. R. Acad. Sci. **176**, 1603 (1923).

[14] W. K. Wooters and W.H. Zurek, Phys. Rev. D **19**, 473 (1979).

[15] For the larger class of *welcher Weg* schemes in which $P_{\rm nonlocal}(p)$ is non-negative, this relation holds for the standard deviation of $P_{\rm nonlocal}(p)$. However, even if positive definite, $P_{\rm nonlocal}(p)$ cannot be interpreted as a distribution for classical momentum kicks unless $W_T(x,p)$ is independent of x.

[16] H.P. Robertson, Phys. Rev. **34**, 163 (1929).

[17] S.M. Tan and D.F. Walls, Phys. Rev. A **47**, 4663 (1993).

[18] M.O. Scully and K. Drühl, Phys. Rev. A **25**, 2208 (1982).

[19] R. Bhandari, Phys. Rev. Lett. **69**, 3720 (1992).

[20] T. Pfau *et al.*, Phys. Rev. Lett. **73**, 1223 (1994).

[21] J.F. Clauser and S. Li, Phys. Rev. A **50**, 2430 (1994).

[22] M.S. Chapman *et al.*, Phys. Rev. Lett. **75**, 3783 (1995).

[23] Indeed, for all values of Kd, there were interference fringes *in real space* at the position of the third grating [J. Schmiedmayer (private communication)], demonstrating the absence of *welcher Weg* information. Rather than the wave number k_g of the gratings, these fringes had a wave number of $k_g+dk_{\rm atom}/2L$, where $k_{\rm atom}$ is the longitudinal wave number of the atom and $2L$ is the total length of the interferometer. This different periodicity, combined with some genuine loss of contrast, caused the variation of the visibility of the fringes in the transmittance of atoms as a function of *grating position*, as determined by Eq. (4.11).

[24] Spontaneous emission can be avoided in atom optics schemes, for example, by choosing the two levels (''excited'' and ''ground'') to be superpositions of nearly degenerate magnetic sublevels. These two levels can still be connected by an optical frequency field by employing the dynamical Stark shift [S. Kunze, K. Diekmann, and G. Rempe, Phys. Rev. Lett. **78**, 2038 (1997)].

[25] P. Storey, M. Collett, and D. Walls, Phys. Rev. A **47**, 405 (1993).

[26] C.S. Adams, M. Sigel, and J. Mlynek, Phys. Rep. **240**, 145 (1994).

[27] Y. Aharonov and D. Bohm, Phys. Rev. **115**, 485 (1959).
[28] M. Peshkin and A. Tonomura, *The Aharonov-Bohm Effect*, Lecture Notes in Physics Vol. 340 (Springer, Berlin, 1989).
[29] T.H. Boyer, Am. J. Phys. **40**, 56 (1972).
[30] H. Fearn, Quantum Semiclass. Opt. **7**, 205 (1995).
[31] R.P. Feynman, R.B. Leighton, and M. Sands, *The Feynman Lectures on Physics* (Addison-Wesley, Reading, MA, 1964), Vol II.
[32] G. Rempe (private communication).